



HAL
open science

Induction of antibiotic specialized metabolism by co-culturing in a collection of phyllosphere bacteria

Shan Shan Qi, Alexander Bogdanov, Margo Cnockaert, Tessa Acar, Sarah Ranty-roby, Tom Coenye, Peter Vandamme, Gabriele König, Max Crüsemann, Aurélien Carlier

► To cite this version:

Shan Shan Qi, Alexander Bogdanov, Margo Cnockaert, Tessa Acar, Sarah Ranty-roby, et al.. Induction of antibiotic specialized metabolism by co-culturing in a collection of phyllosphere bacteria. *Environmental Microbiology*, 2021, 23 (4), pp.2132-2151. 10.1111/1462-2920.15382 . hal-03097074

HAL Id: hal-03097074

<https://hal.inrae.fr/hal-03097074>

Submitted on 5 Jan 2021

HAL is a multi-disciplinary open access archive for the deposit and dissemination of scientific research documents, whether they are published or not. The documents may come from teaching and research institutions in France or abroad, or from public or private research centers.

L'archive ouverte pluridisciplinaire **HAL**, est destinée au dépôt et à la diffusion de documents scientifiques de niveau recherche, publiés ou non, émanant des établissements d'enseignement et de recherche français ou étrangers, des laboratoires publics ou privés.

TITLE: Induction of antibiotic specialized metabolism by co-culturing in a collection of phyllosphere bacteria

AUTHORS:

Shan Shan Qi¹, Alexander Bogdanov², Margo Cnockaert¹, Tessa Acar¹, Sarah Ranty-Roby⁴, Tom Coenye³, Peter Vandamme¹, Gabriele M. König², Max Crüsemann² and Aurélien Carlier^{1,4}

Affiliations

¹ Laboratory of Microbiology, Department of Biochemistry and Microbiology, Faculty of Sciences, Ghent University, Ghent, Belgium

² Institute for Pharmaceutical Biology, University of Bonn, Nussallee 6, 53115 Bonn, Germany

³ Laboratory of Pharmaceutical Microbiology, Ghent University, Ghent, Belgium

⁴ LIPM, Université de Toulouse, INRAE, CNRS, Castanet-Tolosan, France

This article has been accepted for publication and undergone full peer review but has not been through the copyediting, typesetting, pagination and proofreading process which may lead to differences between this version and the [Version of Record](#). Please cite this article as doi: [10.1111/1462-2920.15382](https://doi.org/10.1111/1462-2920.15382)

Abstract

A diverse set of bacteria live on the above ground parts of plants, composing the phyllosphere, and play important roles for plant health. Phyllosphere microbial communities assemble in a predictable manner and diverge from communities colonizing other plant organs or the soil. However, how these communities differ functionally remains obscure. We assembled a collection of 258 bacterial isolates representative of the most abundant taxa of the phyllosphere of *Arabidopsis* and a shared soil inoculum. We screened the collection for the production of metabolites that inhibit the growth of gram-positive and gram-negative bacteria either in isolation or in co-culture. We found that isolates capable of constitutive antibiotic production in monoculture were significantly enriched in the soil fraction. In contrast, the proportion of binary cultures resulting in the production of growth inhibitory compounds differed only marginally between the phyllosphere and soil fractions. This shows that the phyllosphere may be a rich resource for potentially novel molecules with antibiotic activity, but that production or activity is dependent upon induction by external signals or cues. Finally, we describe the isolation of antimicrobial acyloin metabolites from a binary culture of *Arabidopsis* phyllosphere isolates, which inhibit the growth of clinically relevant *Acinetobacter baumannii*.

Introduction

Microbes mostly live in complex communities, whose assembly and structure is dependent on available nutrients, environmental conditions and habitat structure (Cordero and Datta, 2016). In addition, competitive interactions and production of antimicrobial compounds are increasingly recognized as key strategies driving competition and community assembly in microbial habitats (Hibbing *et al*, 2010; Cornforth & Foster, 2013; Granato *et al*, 2019). Production of inhibitory specialized metabolites is thought to play an important role in heterogeneous habitats such as soil, where spatial segregation and high taxonomic diversity create conditions where co-existence of antagonistic genotypes is possible (Cordero and Datta, 2016). Diverse, granular habitats thus hold great promise for the discovery of novel metabolites with medical and biotechnological potential. Indeed, soil has been a historical source of microbes with biotechnological potential and continues to yield novel metabolites of high interest (Ling *et al.*, 2015; Newman and Cragg, 2020). However, the emergence of pathogens resistant to multiple or all antibiotics available in the clinic in the last decades is a cause for urgent concern, with an estimated 700 000 lives lost globally every year to drug-resistant diseases (O'Neill, 2014). Among multi-drug resistant pathogens, a group of 13 taxa

Mycobacterium tuberculosis, *Enterococcus faecium*, *Staphylococcus aureus*, *Acinetobacter baumannii*, *Pseudomonas aeruginosa*, *Helicobacter pylori*, *Streptococcus pneumoniae*, *Haemophilus influenzae*, *Campylobacter* spp., *Salmonella* spp, *Neisseria gonorrhoeae* and carbapenem- & cephalosporin-resistant *Enterobacteriaceae* species, fluoroquinolone-resistant *Shigella* spp) causes the majority of drug-resistant hospital infections (Pendleton *et al.*, 2013; Tacconelli *et al.*, 2018). Of these, carbapenem-resistant *A. baumannii* was listed by the US Center for Disease Control as an urgent antibiotic/antimicrobial resistance threat in 2019 and as a “critical priority” target for research and development of new antibiotics by the WHO (Tacconelli *et al.*, 2018). Carbapenem-resistant *Acinetobacter* cause serious infections in immunocompromised patients and patients in intensive-care units, with some strains being resistant to nearly all antibiotics used in the clinic (CDC, 2019). Along with strategies to limit the spread of antimicrobial resistance, development of novel antimicrobial therapies is critical to mitigate the risks posed by multi-drug resistant infections. The genomes of soil bacteria, for example, contain a wealth of uncharacterized biosynthetic gene clusters (BGCs), harboring great potential for new natural products (Crits-Christoph *et al.*, 2018). However, access to this metabolic diversity is hindered by the fact that specialized metabolism is rarely constitutively expressed. Instead, specialized metabolism is mostly induced by species and sometimes strain-specific cues and signals (Scherlach and Hertweck, 2009). A most promising way to induce the expression of cryptic BGCs is to co-culture microorganisms isolated from the same habitat (Firn and Jones, 2003; Schroeckh *et al.*, 2009). Indeed, several recent studies have highlighted the fact that antibiotic production is more often induced in co-culture than under classical laboratory conditions (Seyedsayamdost *et al.*, 2012; Tyc *et al.*, 2014; Helfrich *et al.*, 2018).

The above-ground parts of plants, composing the phyllosphere, are colonized by a phylogenetically diverse set of bacteria, with fungi a variable and often minor component of microbial communities (Lindow & Brandl, 2003; Vorholt, 2012; Bai *et al.*, 2015). Bacteria colonizing the phyllosphere tend to live in weakly connected micro-habitats that are characterized by a low and uneven concentration of nutrients (Leveau and Lindow, 2001; Miller *et al.*, 2001; Remus-Emsermann *et al.*, 2012, 2014; Schlechter *et al.*, 2019). The phyllosphere is generally understood to act as an ecological filter that selects members of soil and rhizosphere microbiota with some functional traits which are required for life in this environment including the biosynthesis of osmoprotectants, utilization of leaf-specific carbon sources and oligotrophic adaptations (Whipps *et al.*, 2008; Yadav *et al.*, 2008; Hunter *et al.*, 2010; Knief *et al.*, 2012; Bulgarelli *et al.*, 2013; Bai *et al.*, 2015; Levy *et al.*, 2018). In addition, microbe-microbe interactions contribute to shaping phyllosphere communities, but the mechanisms by which they act is poorly understood (Agler *et al.*, 2016; Chen *et al.*, 2020). In particular, microbe-microbe interactions have been linked to community structuring in the phyllosphere, as well as

disease suppression, but the ecological mechanisms leading to selection or enrichment of certain functions in the plant microbiome remain largely uncharacterized (Hunter *et al.*, 2010; Levy *et al.*, 2018; Carrión *et al.*, 2019). This lack of understanding of ecological factors contributes to making the leaf an underexplored environment for the production of specialized metabolites (Helfrich *et al.*, 2018).

To gain insight into the potential of the phyllosphere for the mining of novel specialized metabolites, we assembled a collection of 258 taxonomically diverse isolates from artificially inoculated leaves of *Arabidopsis* and surrounding soil. We screened the isolates for the production of metabolites which inhibited bacterial growth in mono- and co-culture and showed that constitutive production in axenic condition was rare, with most antibiotic synthesis induced exclusively in co-culture. Phyllosphere isolates were significantly less likely to produce inhibitory compounds compared to soil isolates in monoculture, whereas induction in response to sympatric isolates was only marginally affected by isolation source. Similarly, suppression of antibiotic production upon co-culturing was equally common for both soil and phyllosphere isolates, but rarer in co-cultures of strains of different isolation sources. The high taxonomic diversity, relative ease of culturing and the finding that co-culturing is an effective way to screen for antibiotic production in the phyllosphere provide new opportunities for the development of novel natural scaffolds. To illustrate this, we report the isolation of 5 satabacin and xenoclyoin-type antibiotic compounds from a co-culture of *Paenibacillus* and *Sphingomonas* strains, which display toxicity against the gram-negative pathogen *A. baumannii*.

MATERIALS AND METHODS

Source of microbial inoculum

A top soil sample (pH 3.5) was collected in 2015 at 10 cm depth in the Almoeseneie forest (N 50°58'30.1" E003°48'11.2", Gontrode, Belgium). The soil was homogenized, frozen in liquid nitrogen and stored at -80 °C in 250 mL sterile plastic containers (Nalgene, USA).

Plant accessions and culture conditions

Seeds of *Arabidopsis thaliana* Col-0 were surface-sterilized with 1% sodium hypochlorite for 1 min, rinsed and treated by 70% ethanol for 10 min, followed by washing five times with sterile water. In an effort to increase reproducibility of the experiments, we maintained the plants in a closed system to minimize environmental contamination (e.g. through aerial deposits). Sterile Microbox containers (reference OS140+ODS140, SacO2, Belgium) were filled with 90 g of pumice stone substrate (IKEA Vaxer) which had been washed twice in distilled water, twice autoclaved at 121 °C for 20 min and finally dehydrated at 95 °C in the oven for 2-3 days). The pumice stones were hydrated with 60 mL of

0.5x Murashige-Skoog basal medium (Sigma-Aldrich, cat. Number M5519). As a source of inoculum, 10 g of a top soil sample was mixed with 100 mL of autoclaved 0.5x PBS (NaCl 8.0 g/L, KCl 0.2 g/L, Na₂HPO₄ 1.44 g/L, KH₂PO₄ 0.24 g/L) and vortexed for 20 minutes. The suspension was decanted at room temperature for twenty minutes to obtain the soil suspension. 10 mL of this suspension (or 10 mL of 0.5% PBS) was added to each microbox container. Seven seeds per box were sown on top of the substrate and incubated for about 4 weeks in an incubator fitted with LED lights (IKEA L1518) at 21 °C with 50% humidity and a day/night cycle of 12 h. Average light intensity at seed level was approximately 230 μmol·m⁻²·s⁻¹. In addition, three control experiments were performed: 1) same as above but without seeds. 2) same as above (seeds added) but microbial inoculum was omitted and 3) microbial inoculum and seeds were omitted. All experiments were incubated simultaneously, and the pots were shuffled regularly.

Isolation of plant-associated bacteria

Plants were harvested before bolting, 4 weeks after emergence. Shoot-associated bacteria were isolated by collecting above-ground tissue taking care of detaching and discarding leaves that had been in contact with the substrate. Soil samples were collected directly from the growing substrates, taking care not to contaminate the samples with detached plant debris. All samples were transferred in 10 mL 0.5x PBS and sonicated for 20 min. The supernatants were used directly for the isolation of microorganisms. Five mL aliquots were collected, transferred to sterile microfuge tubes and centrifuged for 6 min at 5000 rpm in a benchtop centrifuge. The pellets were immediately frozen and stored at -80 °C until needed for culture-independent analysis.

Microbial suspensions were plated directly without enrichment on a range of general and selective isolation media to maximize recovery of taxa known to colonize plants. The general isolation media used were 10% tryptic soy agar (TSA) (10% tryptic soy broth, Oxoid, Thermo Scientific, 18 g/L agar), Luria Bertani agar (LB) agar (tryptone 10 g/L, yeast extract 5 g/L, NaCl 10 g/L, agar 20 g/L, pH 7), water yeast extract agar (Cuesta *et al.*, 2012) (WYE agar; yeast extract 0.25 g/L, 18 g/L agar, pH 7.2) and ISP2 agar (yeast extract 4 g/L, malt extract 10 g/L, dextrose 4 g/L, agar 20 g/L pH 7.2). Selective isolation media were: *Pseudomonas* isolation agar (Sigma-Aldrich) and 10% PCAT (*Pseudomonas cepacia*, azelaic acid, tryptamine) medium (Peeters *et al.*, 2016) to target pseudomonads and *Burkholderia* sp. For the isolation of sporulating *Bacillales*, aliquots of cell suspensions were treated at 80 °C for 30 min before plating on 10% TSA and LB agar. 30 to 50 μL of decimal serial dilutions (from 10⁻¹-10⁻⁹) for each cell suspension were spread on standard Petri dishes filled with 15 mL-20 mL of media and incubated aerobically at room temperature for 3-7 days. Colonies were picked as they

appeared, streaked out on (TSA) and incubated at room temperature. Strains were passaged 3 times on TSA prior to preservation at -80 °C in tryptic soy broth supplemented with 20% glycerol.

Taxonomic classification of isolates and dereplication

We isolated a total of 3372 colonies. Cell extracts for MALDI-TOF MS profiling were done as described by Dumolin et al. (Dumolin *et al.*, 2019). Briefly, a 1- μ l loopful of bacterial cells was suspended in 300 μ l of Milli-Q water and vortexed to a homogeneous suspension. Next, 900 μ l of absolute ethanol (EtOH) was added, the components were mixed by inversion, and the mixture was centrifuged for 3 min at 4 °C (14,000 rpm). Samples were stored at -20 °C. At the time of analysis, samples were centrifuged as described above, supernatants were discarded, and centrifugation was repeated to remove the residual EtOH, followed by air drying for 5 min at room temperature. The pellet was suspended in 40 μ l of 70% formic acid in water and mixed by vortexing. Finally, 40 μ l of acetonitrile was added and the mixture was vortexed. The extract was centrifuged for 3 min at 4 °C (14,000 rpm) to remove the cell debris, and the supernatant was transferred to a new tube. All liquid handling steps were performed with a Viaflo 96 electronic pipette (Integra Biosystems, Switzerland). Bacterial cell extracts (1 μ l) were spotted on a target plate (Bruker Daltonik, Bremen, Germany) in duplicate and dried in air at room temperature. The sample spot was overlaid with 1 μ l of matrix solution (10 mg/mL α -cyano-4-hydroxycinnamic acid in acetonitrile:water:TFA 50:47.5:2.5). Each target plate comprised one spot of pure matrix solution used as a negative control and one spot of Bacterial Test Standard (Bruker Daltonik, Bremen, Germany) used for calibration. The target plate was measured automatically on the Bruker Microflex™ LT platform (Bruker Daltonik, Bremen, Germany). Spectra were obtained in linear, positive ion mode using FlexControl 3.4 according to manufacturer's recommended settings (Bruker Daltonik, Bremen, Germany). Each final spectrum resulted from the sum of spectra generated at random positions to a maximum of 240 shots per spectrum. The mass spectra were retrieved as t2d files from the 4800 PlusMALDI TOF/TOF™ Analyzer via the 4000 Series Explorer software. Data Explorer 4.0-software (Applied Biosystems, USA) was used to convert the t2d files into text files. Dereplication of mass spectra was done using the SPeDE software with default settings (Dumolin *et al.*, 2019), resulting in 292 clusters of indistinguishable spectra. Representative isolates from each cluster were selected to build a final collection of 258 MALDI-TOF-defined independent strains. Wherever isolates from multiple isolation sources were present in a cluster, care was taken to select a representative of each source. The difference between the number of clusters and the final makeup of the collection was due to our inability to recover some strains from storage.

The final collection of 258 strains was further characterized by 16S rRNA gene sequencing. DNA extraction was performed by using the alkaline lysis method (Niemann *et al.*, 1997). PCR was

performed using primers pA (5'-AGA GTT TGA TCC TGG CTC AG) and pH (5'-AAG GAG GTG ATC CAG CCG CA) and sequencing done at Eurofins Genomics (Ebersberg, Germany) for the 16S rRNA gene sequencing using primer BLK1 (5'-GTATTACCGCGGCTGCTGGCA) and *Gamma (5'-CTCCTACGGGAGGCAGCAGT). Overlapping forward and reverse sequences were assembled in CLC Main Workbench v 8.0 (Qiagen, Aarhus, Denmark) to yield sequences of 1200 bp on average. Final taxonomic identification was done using release 138 of the SILVA database (Table S1) (Quast *et al.*, 2013). The 16S gene sequences have been deposited in the Zenodo database (<http://doi.org/10.5281/zenodo.3978296>).

Culture-independent bacterial 16S rRNA gene profiling

Parts of *A. thaliana* shoots (hereafter phyllosphere samples), substrates (planted soil) and corresponding unplanted substrate (unplanted soil) samples used for bacterial isolation were also processed for bacterial 16S rRNA gene community profiling using Illumina sequencing. Entire shoots cut above the crown were submerged in sterile 10 mL of 0.5 x PBS buffer and sonicated for 30 min at room temperature in a Branson 3200 ultrasonic bath. Soil samples were processed in an identical fashion. Homogenized soil or plant material was resuspended in lysis buffer of the MO BIO PowerSoil DNA isolation Kit (MO BIO Laboratories Inc., Carlsbad, CA, USA), transferred into lysis matrix tubes provided with the kit, and DNA extraction was performed following the manufacturer's protocol and using a Retsch MM400 mill. DNA concentrations were measured using a Quantus fluorimeter and a QuantiFluor One double-stranded DNA kit (Promega), and subsequently diluted to 30 ng/μl when appropriate. Bacterial 16S rRNA genes were subsequently amplified using PCR primers 341F (5'-CCTAYGGGRBGCASCAG-3') and 806R (5'-GGACTACHVGGGTWTCTAAT-3') targeting the V3-V4 region of the bacterial 16S rRNA gene (Table S1). Each sample was amplified in triplicate by two independent PCR mixtures (a total of 6 replicates per sample plus respective no template controls). PCR products of triplicate were pooled and purified. 250 bp paired-end sequencing libraries were prepared using NEBNext® Ultra™ II DNA Library Prep Kit according to the manufacturer's recommendations. Illumina paired-end sequencing was performed on Illumina HiSeq 2500 at Novogene (Co., Ltd, China). Sequencing reads were filtered and trimmed using Trimmomatic 0.33 (Bolger *et al.*, 2014) in paired-end mode to remove leftover sequencing adapters and clipping reads below Q20. Sequencing reads were imported in QIIME 2 (Bolyen *et al.*, 2018), denoised and merged using DADA2 (Callahan *et al.*, 2016) as implemented in QIIME 2. Primer sequences were removed by calling DADA2 with the following parameters: --p-trim-left-f = 23, --p-trim-left-r = 26. After filtering, the most rarefied sample contained >14 000 non-chimeric merged read pairs. Amplicon sequence variants (ASV) were collected in a table following the DADA2 pipeline instructions. Taxonomy was assigned based on the SILVA reference database v.132 using the naïve Bayes classifier routine

implemented in QIIME 2. ASVs representing chloroplasts and mitochondria were removed from downstream analyses. Additionally, ASVs occurring in the “no template” control at frequencies >0.1% and found in less than 8 samples were removed from downstream analyses. 576 ASVs across all samples remained after filtering. Data analyses were done in R using the *phyloseq* package (McMurdie and Holmes, 2013; R Core Team, 2014). ASV table and sequences are deposited on Zenodo (<http://doi.org/10.5281/zenodo.3978296>).

Whole genome shotgun sequencing and annotation

Genomic DNA was extracted using a CTAB/phenol-chloroform method (Wilson, 2001) or using a Maxwell 16 tissue DNA purification kit (Promega, Madison, WI, USA). Gram-positive bacterial cultures were incubated with 5 mg of lysozyme (Serva, Germany) and 40 μ l mutanolysin (5,000 U/ml; Sigma) dissolved in 110 ml of TE buffer (10 mM Tris Cl, 1 mM EDTA). DNA integrity and purity were evaluated on a 1.0% (wt/vol) agarose gel and by spectrophotometric measurements at 234, 260, and 280 nm. A Quantus fluorimeter and a QuantiFluor One double-stranded DNA system (Promega) were used to measure the DNA concentration. Paired-end 2x150 bp libraries were prepared at the Wellcome Trust Human Genome Center (Oxford, UK) using the NEBNext DNA library kit for Illumina (New England Biolabs, Ipswich, MA, USA) and sequenced on an Illumina HiSeq 4000 instrument. Sequencing reads were prepared for assembly by adapter trimming and read filtering using Trimmomatic (Bolger *et al.*, 2014). Reads with phred scores below 30 were removed and non-paired reads were discarded. Genome size and average base coverage was estimated by k-mer counting using Jellyfish (Marçais and Kingsford, 2011). Reads were subset to give an approximate coverage of 100x and assembled using SPAdes v3.10.1 (Bankevich *et al.*, 2012) with kmer-lengths of 21, 33, 55, 77, 99 and 121 or with Skesa (Souvorov *et al.*, 2018) using default settings. Short contigs (< 500 bp) or with < 50% of average genome coverage were removed. To rule out possible contamination or mislabelling of samples, 16S rRNA gene sequences were extracted from the assembled genomes using Barrnap v0.6 (<https://github.com/tseemann/barrnap>) and compared to available sequences for the strain. Biosynthetic gene clusters were predicted using the AntiSMASH web service (Blin *et al.*, 2019). Genomes were compared to the reference genomes of type strains using the TYGS web server (Mukherjee *et al.*, 2017). Genome assemblies and annotations can be downloaded from NCBI Genbank with accession numbers NZ_WHOB000000000 (strain P3_m116_1, also deposited in the BBCM/LMG Bacteria Collection as *Paenibacillus* sp. LMG 31459) and JACCFG000000000 for *Sphingomonas* sp. P2_m126_1 (syn. R-74633).

Sequence and phylogenetic analyses

16S rRNA sequences or ASV sequences were aligned using MAFFT in “auto” mode (Kato and Standley, 2013). Alignments were edited and trimmed with Trimal (Capella-Gutiérrez *et al.*, 2009). Alignments were used to create approximate maximum likelihood phylogenetic trees using FastTree 2 software with the GTR model (Price *et al.*, 2010). To match ASV sequences to isolates, the sequences of the 100 most abundant ASVs per condition and plant site were extracted and searched using BLASTn (Altschul *et al.*, 1990) against a database of partial 16S rRNA sequences of our isolates (including the V3-V4 region). Alignments resulting in identity over a threshold value (either 99% or 97%) over the entire length of the alignment were considered as evidence of similarity between an ASV and a 16S rRNA gene sequence.

Bipartite growth inhibition screen

We screened our collection of isolates for the production of antimicrobial compounds in mono- and co-cultures against two model organisms commonly used in drug discovery: *S. aureus* LMG 10147 (syn. ATCC 29213) (Soni *et al.*, 2015) and *A. baumannii* LMG 10520 (syn. RUH 112) (Janssen *et al.*, 1997). We applied an antimicrobial antagonism overlay assay because it is specific for the detection of diffusible metabolites (Abrudan *et al.*, 2015). The method was adapted from (Mahenthiralingam *et al.*, 2011). Briefly, individual strains were grown overnight, 3 μ L of cultures were spotted on the surface of a Petri dish containing 15 mL of 100% TSA medium and incubated for 4 days at 21 °C (Figure S1). For tests in co-culture, a drop of 3 μ L of each culture was spotted sequentially on the surface of the agar. Some isolates grew poorly in these conditions and were left out of the experiment, resulting in data collected from 224 isolates only. After initial incubation for 4 days, a soft agar layer was poured over the cultures, using 10 mL of soft agar (ISB supplemented with 10 g/L agar) containing an inoculum of either *A. baumannii* LMG 10520 or *S. aureus* LMG 10147 (100 μ L of overnight culture per 100 mL of broth), and supplemented with 2,3,5-triphenyl tetrazolium chloride (0.1 g/L final concentration). Because testing all combinations of isolates in inhibition assays against 2 test organisms would have resulted in an unmanageable number of assays, we focused on a random sampling strategy and tested about 10 000 strain combinations per test strain (out of the nearly 50 000 possible combinations). Most strain combinations were tested against both test strains (8984/9358 combinations tested with *A. baumannii* were also tested with *S. aureus*; and 9042/10285 combinations tested against *S. aureus* were also tested against *A. baumannii*). Each strain appeared on average 164 times in the screen, with a maximum of 301 times. After air-drying the plates for 5 min under a laminar flow, a 15 mL overlay consisting of soft agar containing the test organism was poured over the culture. The overlay consisted of soft Iso-Sensitest agar (Oxoid Iso-Sensitest broth 23.4g/L, Oxoid agar no.1 10 g/L, pH 7), autoclaved for 20 min at 121 °C and cooled to ca. 37 °C. The overlay medium was supplemented with filter-sterilized 2,3,5-triphenyl tetrazolium chloride (TTC,

0.1 g/L) and an overnight culture of the test organism in ISB medium to a final dilution of approximately $OD_{590nm} = 0.002$ for *A. baumannii* LMG 10520 and 0.01 for *S. aureus* LMG 10147. Cultures were incubated at 37 °C and the inhibition zones were scored after 24 h. We used scoring schemes adapted to the different phenotypes of the test organisms. For *S. aureus* LMG 10147, a score of 0 indicated no visible clearing or only a light discoloration around the colony; a score of 1 indicated strong discoloration with a halo of > 2 mm around the colony or total clearing > 1 mm. A score of 2 indicated complete clearing > 2 mm around the colony. For *A. baumannii* LMG 10520, a score of 0 indicated no clearing, a score of 1 indicated clearing wider than 1 mm around the colony and a score of 2 indicated complete clearing > 2 mm around the colony (Figure S2). Combinations which resulted in a clearing zone or halo formation were checked in duplicate.

Isolation of antimicrobial compounds and chemical characterization

After 7 days of incubation at room temperature, agar with bacterial colonies (P3_m116_1 and P2_m126_1) was transferred from the standard plastic petri dishes (162 in total) to 2 L glass beakers, crushed, submerged with dichloromethane, and sonicated for around 40 minutes in a Branson 3200 ultrasonic bath. The liquid was filtered through a funnel plugged with glass wool and evaporated under reduced pressure to yield crude extract. The extraction procedure was repeated three times. Dry extracts were then preserved at -20 °C for further analyses. Afterwards, the crude extract (534.5 mg) was re-suspended in 20:80 MeOH:H₂O and fractionated with vacuum liquid chromatography (VLC) over a Polyogoprep 60-50 reversed phase C₁₈ stationary phase using a stepwise gradient (20:80, 40:60, 60:40, 80:20, 100:0 MeOH:H₂O v/v, 100 mL each) to obtain six fractions. Final fraction 7 was eluted with 100 mL 90:10 MeOH: acetone. VLC fractions were submitted to antibacterial testing, which was performed at 2 mg (0.1 mg/ul). The most active fraction VLC5 (55 mg) was further separated on HPLC using a Nucleodur C₁₈ 5 µm Pyramid 250 mm x 10 mm column and isocratic 70:30 MeOH/H₂O mobile phase at 2.5 mL/min flow to yield 5 pure compounds **1** (7.3 mg), **2** (4.3 mg), **3** (1.3 mg), **4** (3.5 mg) and **5** (2.0 mg). NMR spectra were recorded in MeOH-*d*₄ using a Bruker Avance 300 DPX spectrometer. Spectra were referenced to residual solvent signals with resonances at $\delta_{H/C}$ 3.35/49.0. Mass spectra were recorded on a micrOTOF-QIII mass spectrometer (Bruker) with ESI-source coupled with a HPLC Dionex Ultimate 3000 (Thermo Scientific) using an EC10/2 Nucleoshell C₁₈ 2.7 µm column (Macherey-Nagel). The column temperature was 25 °C. MS data were acquired over a range from 100-3000 *m/z* in positive mode. Auto MS/MS fragmentation was achieved with rising collision energy (35-50 keV over a gradient from 500-2000 *m/z*) with a frequency of 4 Hz for all

ions over a threshold of 100. HPLC begins with 90 % H₂O containing 0.1% acetic acid. The gradient starts after 1 min to 100% acetonitrile (0.1% acetic acid) in 10 min. A 5 µL amount of a 1 mg/ml sample solution (MeOH) was injected at a flow of 0.3 mL/min. All solvents were LCMS grade. Preparative HPLC was performed on a Merck Hitachi HPLC system equipped with a L-6200A pump, a L-4500A PDA detector, a D-6000A interface with D-7000A HSM software, a Rheodyne 7725i injection system. A Nucleodur C₁₈ 5 µm Pyramid 250 mm x 10 mm (Macherey-Nagel) column was used.

Determination of minimum inhibitory concentrations (MIC)

Determination of the MIC of the isolated acyloin compounds was based on the method described by Alderman and Smith (Alderman and Smith, 2001). Briefly, overnight cultures of clinical isolates of *A. baumannii* in ISB were diluted with fresh ISB liquid medium to a final OD₅₉₀=0.001 (approximately 1.0x10⁶ cfu/ml as determined with *A. baumannii* RUH 0134, data not shown). Two-fold dilution series of the test compounds were made in ISB medium. Fifty µL of these solutions were added to 96-well plates, to which 50 µL of the test strain suspension were added. The cultures were incubated at 37 °C for 24 h and wells where no growth occurred were determined by eye. The concentrations of compounds tested ranged from 1 µg/ml to 128 µg/mL in 2-fold stepwise increments. The strains tested included: *A. baumannii* 70pus (OXA-24 like carbapenem-resistant, received from H. Goossens, Department of Medical Microbiology, University of Antwerp, Belgium), *A. baumannii* RUH 0134 (Janssen *et al.*, 1997), multidrug resistant *A. baumannii* NCTC 13423 (Turton *et al.*, 2006), *A. baumannii* RUH 3247 (Dijkshoorn *et al.*, 1996), *A. baumannii* LUH 3788 (Nemec *et al.*, 2004), and *A. baumannii* A1392 (deposited in the BCCM/LMG collection as strain LMG 22461, (Huys *et al.*, 2005)).

Statistical analyses

All statistical analyses were done in the R environment (R Core Team, 2014). Scripts and data are available from <https://github.com/CarrierLab/bipartite-interactions-phylosphere-arabidopsis>

RESULTS

Assembly of a collection of bacteria associated with the phyllosphere of *Arabidopsis*

To gain insight into the metabolic potential of plant-associated communities, and the phyllosphere in particular, we designed an experiment in which an inert, sterile substrate (pumice stone) was inoculated with a soil suspension and planted with *Arabidopsis thaliana*. *Arabidopsis* seedlings grown in that medium under otherwise gnotobiotic conditions were harvested before the bolting stage after 4 weeks of incubation. We isolated bacteria on a range of selective and non-selective media and growth conditions to target taxa known to be prolific specialized metabolite producers:

Bacillales, *Actinomycetes*, pseudomonads and *Burkholderiales* in addition to general chemoheterotrophic bacteria. We isolated epiphytic bacteria from whole shoots cut above the soil line (hereafter phyllosphere samples) (Figure 1). We also isolated bacteria from the pumice substrate which was inoculated with the soil suspension but in which no plants had been sown (soil samples), as well as from uninoculated, unplanted pumice substrate (pumice samples). In total, we isolated about 3300 colonies from the various samples and culture conditions (1481 from phyllosphere samples, 1844 from soil and 47 from pumice). Isolates were dereplicated using MALDI-TOF MS profiles and the SPeDE software to yield 292 unique profiles. To build the culture collection, we picked one representative isolate per cluster. If a cluster contained isolates with multiple isolation sources (e.g. both phyllosphere and soil), we picked one representative per isolation source. Of the isolates which survived passaging and storage at -80 °C, 161 were isolated from phyllosphere samples, 91 from soil and 6 from pumice. We obtained partial 16S rRNA sequences for 244 of these isolates (Table S1). Our collection is composed of 59% *Proteobacteria*, 21% *Actinobacteria*, 12% *Firmicutes* and 7% *Bacteroidetes* (Figure S3). The most abundant families are *Pseudomonadaceae* (22.1%) followed by *Paenibacillaceae* (11.1%), *Microbacteriaceae* (8.1%), *Sphingobacteriaceae* (6.1%), *Burkholderiaceae* (6.1%), *Xanthomonadaceae* (6.1%) and *Rhizobiaceae* (5.7%).

In parallel, we performed cultivation-independent 16S rRNA gene profiling to cross-reference taxa from the microbiota with individual isolates. Communities from the phyllosphere were distinct from those in unplanted soil and planted soil, while communities from planted and unplanted soil overlapped (Figure S4). We also observed a richness gradient between the different compartments, with the unplanted soil samples having on average higher alpha diversity values than planted soil and the phyllosphere. This difference in richness was significant between the phyllosphere and the other samples, but not between planted and unplanted soil (Figure S4). Despite these differences, we found significant overlap between bacterial communities of the phyllosphere and unplanted soil, with 51 of the top 100 most abundant ASVs shared between the two compartments (Figure 2).

To assess the degree of representation and recovery of our isolate collection, we compared 244 near full-length 16S rRNA gene sequences of our collection to the most abundant ASVs from the phyllosphere, soil and pumice samples. With a sequence similarity cut-off of 99%, we recovered 49/152 of the top 100 most abundant ASVs across all three habitats in our collection. Recovery of top 100 ASVs was 38% for the phyllosphere samples, 39% for the soil and 36% for pumice (Figure 3). At 97% identity, we recovered 52% and 48% of the top 100 ASVs from the phyllosphere and soil communities, respectively.

Estimating the biosynthetic potential of *Arabidopsis* shoot microbiota

Plant microbiota are a potential source of novel antimicrobial specialized metabolism (Bangera, 1996; Lu and Shen, 2003; Dandurishvili *et al*, 2011; Helfrich *et al*, 2018). To determine if the bacteria colonizing the different plant compartments are enriched in antimicrobial metabolism and if their antagonistic strategies differ, we screened our collection for inhibitory activity in an overlay assay against two test organisms: *S. aureus* LMG 10147 and *A. baumannii* LMG 10520. We reasoned that these test strains, which were isolated from environments other than soil and plants, would be less likely to have evolved resistance mechanisms to antibiotics produced by organisms in our collection therefore mitigating potential biases in the detection. Both test organisms are nosocomial pathogens that exhibit varying levels of multidrug resistance and virulence. We first tested single isolates against both test organisms. Because some isolates grew poorly or slowly on TSA medium, we tested only 224 strains of our collection. Of these, 27 inhibited growth of *S. aureus* in monoculture and one that of *A. baumannii*, albeit weakly (Table 1). We named these strains monoculture-producers. Monoculture-producers belonged to only 4 genera: *Pseudomonas* (24 strains), *Streptomyces* (2 strains), *Paenibacillus* (1 strain) and *Staphylococcus* (1 strain). Of these, 8 strains had been isolated from the phyllosphere and 20 from soil. The soil compartment is thus significantly enriched in strains which constitutively produce antibiotics compared to the phyllosphere compartment (21.9% vs 4.9%, Chi-square test $p < 0.001$).

Selective induction of antibiotic production as a response to co-culture only marginally differs between phyllosphere and soil isolates of the collection

Because only a fraction of natural product BGCs are expressed in axenic cultures (Tyc *et al*, 2014; Helfrich *et al*, 2018), we tested randomly selected, pairwise combinations of strains for growth inhibition of *S. aureus* LMG 10147 and *A. baumannii* LMG 10520 to get a more representative view of the biosynthetic potential of our collection. In total, we tested 9358 and 10221 unique combinations for inhibitory activity against *A. baumannii* and *S. aureus*, respectively (Table S2).

First, we considered only co-cultures between strains which did not display constitutive inhibitory activity in monoculture. Inhibitory interactions are rare, with only 121 unique combinations resulting in inhibitory activities against *A. baumannii* LMG 10520 and 107 against *S. aureus* LMG 10147, or 1.29% and 1.05% of all interactions tested, respectively (Table 2, Table S2). Moreover, the distribution is skewed: the top 5 strains are involved in 48.5% and 40.2% of inhibitory interactions against *S. aureus* and *A. baumannii*, respectively. Taken together, 1.20% (78/6492) of interactions with growth inhibitory activity involved pairs of phyllosphere isolates, 2.20% (33/1496) involved pairs of soil isolates and 1.72% (115/6671) were between a phyllosphere and a soil isolate. The proportion

of interactions resulting in growth inhibition was 1.83x higher between strains sharing a soil habitat than for strains of the phyllosphere (Pearson Chi-squared test with Yates' continuity correction p -value = 0.004). This trend was preserved when we considered the inhibitory activity against *A. baumannii* LMG 10520 separately: phyllosphere-phyllosphere co-cultures resulted in 0.89% and soil-soil co-cultures in 2.85% of inhibitory interactions (Chi-squared test $p < 0.001$). However, the number of co-cultures with inhibitory activity against *S. aureus* LMG 10147 was not significantly different when both isolates came from the phyllosphere or when both came from soil (1.52% vs. 1.63%, respectively; Pearson Chi-squared test p -value = 0.94). We did not observe any significant correlation between the phylogenetic distance between isolates and the capacity to produce antibiotics in co-culture (Figure S5). Together, these data show that activation of specialized metabolism by microbe-microbe interactions is only marginally more common in the soil than in the phyllosphere and that activation is independent of the broad taxonomic makeup of plant-associated microbial communities. Furthermore, the node degree distributions between the interaction networks of phyllosphere vs. soil isolates are not significantly different once monoculture-producers are removed from the network (Figure 4, Kolmogorov-Smirnov test $p = 0.26$). This indicates that there is no difference in the type of response to co-culturing between phyllosphere or soil isolates.

Few taxa are responsible for most growth inhibition in co-culture

Similar to what we observed in monocultures, a few taxa dominated the network of binary interactions resulting in antibiotic production (Figure 3, Figure S6). Members of the *Pseudomonadaceae* were involved in more than 91% of co-cultures which produced antibiotics active against *S. aureus* LMG 10147. Conversely, pairs of strains active against *A. baumannii* LMG 10520 comprised at least one member of the *Paenibacillaceae* in 62% of cases or a *Micrococcaceae* in 49% of cases. Interestingly, a few taxa, while not harboring probable antibiotic producers (i.e. strains involved in more than 1 inhibitory interaction), contained strains capable of inducing antibiotic production in all major groups (Figure S6). For example, the 4th node with the highest degree in the interaction network (Figure S6) represented strains of the family *Sphingobacteriaceae* (phylum *Bacteroidetes*). These strains were nearly exclusively isolated from the phyllosphere (Figure 3) and were capable of inducing antibiotic production with all the major producing taxa *Pseudomonadaceae*, *Paenibacillaceae* and *Micrococcaceae*.

Widespread suppression of growth inhibition upon co-culturing

In addition to the two behaviors described above (antibiotic production induced in monoculture vs. co-culture), some monoculture producers did not display inhibition against *S. aureus* LMG 10147 in co-culture with other isolates. We tested a total of 2269 pairwise interactions (a subset of the 6244

possible combinations) involving a monoculture producer (Figure S7). The frequency of this suppressive behavior did not significantly differ between phyllosphere-phyllosphere isolates in co-culture (180/600 or 30.0% of interactions) or soil-soil co-cultures (119/420 or 28.3%; Chi-squared test $p = 0.6$). Soil-phyllosphere combinations displayed significantly lower suppression rates compared to soil-soil or phyllosphere-phyllosphere co-cultures, with 22.5% of interactions showing suppression (Chi-squared test $p < 0.05$). Again, suppression did not correlate with phylogenetic distance between strains in co-culture (Mann-Whitney test p -value > 0.05 , not shown).

Suppression of *S. aureus* growth inhibition displayed limited strain-specificity, with monoculture producers suppressed by 21.5 strains on average (Figure S7). Similarly, strains which suppressed antibiotic production often did so with multiple monoculture producers (median = 2, average = 3.6). Co-cultures between 2 monoculture producers also sometimes resulted in a loss of inhibitory activity. The number of co-cultures of a given strain with another monoculture producer resulting in loss of antibiotic activity ranged from 0 to 9, but the number of suppressive interactions scaled with the number of interactions tested (Figure S7), indicating that suppression of antibiotic production between producers is widespread. No clear pattern emerged regarding taxonomic distribution of suppressive interactions (Figure S8). Only *Pseudomonadaceae* were displayed as a highly connected node on a network of suppressive interactions, but this was also the taxon with the most constitutive antibiotic producers in our assay.

Isolation of antibiotic metabolites from co-cultures of phyllosphere isolates

This complex interplay between induction and suppression of antibiotic production highlights the potential of the phyllosphere as an underexplored and potentially rich environment for new antibiotic leads, especially for metabolites that are not expressed in monoculture on standard microbiological media. We selected a combination of two strains (P3_m116_1 and P2_m126_1) which were able to inhibit the growth of *A. baumannii* LMG 10520. In addition, we tested this combination against a panel of 6 strains representative of multidrug-resistant pathogens: *E. faecium* LMG 16003, *S. aureus* ATCC 700699, *A. baumannii* 70pus (a carbapenem-resistant nosocomial isolate), *Enterobacter cloacae* MI13035761-2, *K. pneumoniae* LMG 29428 and *P. aeruginosa* LMG 6395). Extracts of the P3_m116_1 & P2_m126_1 co-cultures did not show activity against any of the six strains except *A. baumannii* 70pus, indicating the potential for compounds produced by the co-culture for specific activity against *A. baumannii*. With genome-wide average nucleotide identity values are below 95% with other type species of the genus *Paenibacillus*, strain P3_m116_1 (LMG 31459) may represent a novel species which we tentatively named *Paenibacillus phytohabitans* (Qi et al., *in press*). Strain P2_m126_1 belongs to the genus *Sphingomonas* and is closely related to the

species *Sphingomonas kyeonggiensis* (with 98.5% similarity at the 16S rRNA level and genome-wide sequence identity dDDH = 30.2%). Both strains are involved in multiple inhibitory interactions in our co-culture screening assays (Figure 4), however co-cultures with strain *Paenibacillus* sp. P3_m116_1 exclusively produce inhibitory compounds against *A. baumannii* LMG 10520 (26 interactions in total), while strain *Sphingomonas* sp. P2_m126_1 is involved in inhibitory activity against both *S. aureus* LMG 10147 (3 interactions) and *A. baumannii* LMG 10520 (3 interactions). *Paenibacillus* sp. P3_m116_1 is thus the most likely source of the inhibitory metabolite(s) detected in co-culture with *Sphingomonas* sp. P2_m126_1.

In addition, the genome of *Sphingomonas* sp. P2_m126_1 does not encode enzymes commonly involved in antibiotic biosynthesis such as non-ribosomal peptide synthetases (NRPS) or polyketide synthases (PKS) and only one putative lasso peptide locus (data not shown). Conversely, the genome of *Paenibacillus* sp. P3_m116_1 encodes multiple, uncharacterized BGCs: three NRPS or NRPS-like gene clusters, two putative trans-AT PKS clusters, in addition to a cluster with high homology to the recently described non-antimicrobial lassopeptide paeninodin biosynthetic genes (Zhu *et al.*, 2016). To identify the metabolites responsible for the antibiosis against *A. baumannii* LMG 10520, strains *Paenibacillus* sp. P3_m116_1 and *Sphingomonas* sp. P2_m126_1 were grown in co-culture in a large scale on a solid medium (162 petri-dishes) and extracted with dichloromethane. Bioassay-guided fractionation using vacuum liquid chromatography (VLC) and reversed phase HPLC of the active fraction VLC5 yielded five candidate metabolites responsible for the antibiotic activity, i.e. satabacin derivatives (2S,4S)-2-hydroxy-4-methyl-1-phenylhexan-3-one (**1**), (2S,3S)-4-methyl-1-phenylpentane-2,3-diol (**2**) and indole derivatives xenocloins A, B and D (**3–5**) (Figure 5, Figure S9). The structures of known natural products **2–5** were established by analysis and comparison of the ¹H, ¹³C NMR and MS spectra with literature data (Aronoff *et al.*, 2010; Jiang *et al.*, 2019; see Supplementary Information). However, the NMR shifts of compound **1** differed from any of the previously published molecules. Overlapped resonances of protons (δ H 7.30 and 7.24) and six deshielded carbon resonances indicated a phenyl ring bearing one aliphatic substituent similar as found in satabacin-type compound **2**. The remaining carbon resonances included one carbonyl, two methines, two methylenes and two magnetically unequal methyls. These signals were assigned to the acyloin side chain and were almost identical to those of xenocloin B (**4**) except the ¹³C resonance of the methylene adjacent to the ring moiety is shifted downfield (40.8 ppm in **1**, 30.7 ppm in **4**). We report (2S,4S)-2-hydroxy-4-methyl-1-phenylhexan-3-one (**1**) as a natural product for the first time. Due to similar biosynthetic pathways, the absolute configuration of isolated compounds is assumed to be the same as reported in the literature (Aronoff *et al.*, 2010; Jiang *et al.*, 2019).

Both sattabacin and xenocycloin molecules are assembled by thiamine diphosphate (TPP)-dependent enzymes, termed acylain synthases (Proschak *et al*, 2014; Park *et al*, 2014; Schieferdecker *et al*, 2019). Sattabacins are formed by a ligation of phenylpyruvate precursors with 2-oxo valeric acid derivatives, while xenocycloins are synthesized by employing indole pyruvate precursors instead. We therefore searched for homologues of the known acylain synthases Thzk0150 and XclA in the genome of *Paenibacillus* sp. P3_m116_1. The CDS with locus tag GC101_RS07275 lies within a putative operon with a gene encoding a carboxymuconolactone decarboxylase homologue (GC101_RS07280) and a 3-oxoacyl ACP synthase III homologue (GC101_RS07290). These functions are also encoded in the xenocycloin BGC (MIBIG accession number BGC0000189) and are hypothesized to catalyze the decarboxylation of the biosynthetic intermediate and O-acylation, respectively (Proschak *et al*, 2014; Schieferdecker *et al*, 2019) (Figure 5). Therefore, we postulate that this BGC is responsible for the production of **1-5**.

We tested antimicrobial activity of **1-5** towards *A. baumannii* LMG 10520 in a disk diffusion assay using 0.2 mg of compound per disk. Of the five compounds, only compound **1** resulted in a clearing, while no growth inhibition was observed for **2-5** (data not shown). We also evaluated the MIC of the compounds **1**, **2** and **4** against a panel of clinical *A. baumannii* strains (Table 3). For nearly all strains the MIC values were below 32 µg/ml for **2** and **4** (sattabacin-like and xenocycloin B, respectively). Surprisingly, **1** inhibited growth of *A. baumannii* LMG 10520 only at concentrations > 128 µg/mL, and did not show activity in liquid broth against the other *A. baumannii* strains (highest concentration tested 128 µg/mL, not shown). This contrasts with the results of the disk diffusion assay and may be due to instability of the compound in aqueous solvent, or to a different sensitivity of *A. baumannii* to the compound on solid vs. liquid medium.

DISCUSSION

Biological interactions, among them competition, are one of the main drivers of microbial community assembly and structure in natural ecosystems (Chaffron *et al*, 2010; Barberán *et al*, 2012; Faust *et al*, 2012; Faust & Raes, 2012; Kurtz *et al*, 2015; Guidi *et al*, 2016; Cordero & Datta, 2016; Ma *et al*, 2016). This realization, combined with a dire need for new antibiotic scaffolds, has led to a renewed interest for natural product discovery in understudied or under-sampled taxa or microbial habitats. Recent studies using *in silico* and taxonomy-guided approaches have revealed the diversity of BGCs or specialized metabolites in plant-associated communities which may mediate biocontrol activities (Grubbs *et al.*, 2017; Blair *et al.*, 2018; Carrión *et al.*, 2019). The sampling of previously underexplored ecosystems has in turn led to the discovery of novel lipodepsipeptides and darobactin from insect

microbiomes (Ganley *et al.*, 2018; Imai *et al.*, 2019), lobatamides from a plant symbiont (Ueoka *et al.*, 2020), or lugdunin from the human gut microbiota (Zipperer *et al.*, 2016). Inspired by these studies, and our own realization that specialized metabolism forms the basis of several obligate bacterial leaf symbioses (Sieber *et al.*, 2015; Carlier *et al.*, 2016; Pinto-Carbó *et al.*, 2016, 2018; De Meyer *et al.*, 2019; Hsiao *et al.*, 2019), we hypothesized that the above-ground surfaces of plants could provide rich and underexplored opportunities for the discovery of novel bioactive metabolites. The phyllosphere in particular hosts taxonomically diverse communities and harbors a majority of culturable taxa (Kinkel, 1997; Whipps *et al.*, 2008; Bai *et al.*, 2015; Massoni *et al.*, 2019). In addition, habitat fragmentation and the weakly connected communities, which characterize the phyllosphere, are ideal conditions for the stabilization of taxonomic or functional diversity.

Similar to other studies (Bodenhausen *et al.*, 2013; Maignien *et al.*, 2014; Bai *et al.*, 2015; Tkacz *et al.*, 2020), we also found that communities from the phyllosphere were distinct from those in unplanted soil and planted soil, while communities from planted and unplanted soil overlapped (Figure S4). Despite these differences, we found significant overlap between bacterial communities of the phyllosphere and unplanted soil, with 51 of the top 100 most abundant ASVs shared between the two compartments (Figure 2). These results recapitulate findings from studies of natural plant-associated communities (Bodenhausen *et al.*, 2013; Bulgarelli *et al.*, 2013; Maignien *et al.*, 2014; Bai *et al.*, 2015; Copeland *et al.*, 2015). Our experimental design, combined with MALDI-TOF MS-guided isolate dereplication, allowed us to compare directly large representative sets of strains isolated from the phyllosphere of *Arabidopsis* and planted substrate. The taxonomy of the recovered isolates is consistent with previous studies (Bai *et al.*, 2015), even if the relative proportions at the phylum and family levels differ slightly. For example, the phyllosphere bacteria collection of Bai *et al.* contained 60.6% of *Proteobacteria*, 28.7% of *Actinobacteria*, 7.1% of *Bacteroidetes* and 3.5% of *Firmicutes*. Their rhizosphere collection contained 66.0% of *Proteobacteria*, 27.2% of *Actinobacteria*, 1.9% of *Bacteroidetes* and 4.8% of *Firmicutes*. In comparison, our collection is enriched in members of the *Firmicutes* and *Bacteroidetes*. These 2 phyla were particularly enriched in our phyllosphere isolate collection (19.0% and 11.2% of the total phyllosphere isolates, respectively, versus 3.4% and 1.1% of the soil isolates).

We could recover isolates corresponding to 52% and 48% of the top 100 ASVs from the phyllosphere and soil communities, respectively. These levels are comparable to those reported by Bai *et al.*, who recovered 54% of leaf communities and 52-64% for root communities (Bai *et al.*, 2015). For comparison, 190/244 of our isolates shared similar 16S rRNA sequences (>97% identity) with isolates of the At-Sphere collections assembled by Bai *et al.* The overlap is highest with the At-L-Sphere collection, which regroups isolates of *Arabidopsis* phyllosphere collection, with 146/244 isolates with

similar 16S rRNA gene sequence in our collection. Of the 53 isolates that were unique to our collection, 10 belonged to the family *Sphingobacteriaceae*, 9 to the *Paenibacillaceae* and 14 to the *Actinobacteria* families *Microbacteriaceae*, *Micrococcaceae* and *Nocardiaceae*. These differences in recovery of specific taxa may reflect a difference in the isolation strategies adopted in the two studies rather than differences in microbiota composition. Overall, the significant overlap between our collection and the At-Sphere collections highlights both the degree of conservation of *Arabidopsis* microbiota and the selectiveness of the leaf as a habitat. While the recovery rate of top 100 most abundant ASVs is high overall, it is taxonomically biased. For example, we failed to isolate any representative of the ASVs associated with the order *Clostridiales* (Figure 2). *Clostridia* are often obligate anaerobes and their isolation requires specific methods not used here or in the Bai et al. study (Rainey, 2015). Because the phyllosphere and rhizosphere are oxic environments, it is however unclear if *Clostridia* are active contributors of the plant microbiota or if the corresponding ASVs correspond to dormant spores carried over from soil. Moreover, some taxa are difficult to resolve with MALDI-TOF MS profiling (e.g. some *Burkholderia* or *Bacillus* species) or with 16S rRNA gene sequencing (Dumolin *et al.*, 2019). As with all strain dereplication strategies, some bias in sub-species diversity is inevitable. Since the representative strains for each dereplication cluster were selected at random, representation biases should not affect the overall conclusions of this study.

We screened our collection of isolates in a tri-partite overlay assay against *S. aureus* and *A. baumannii* strains. We reasoned that clinical isolates would be less likely to have evolved resistance mechanisms to antibiotics produced in soil or plant-associated niches, mitigating potential biases in detection. In our phylogenetically diverse collection of plant-associated bacteria, only 11.8% displayed any ability to inhibit the growth in pure culture of *S. aureus* or *A. baumannii* strains used in our screen. These isolates belonged to taxa well known for the production of specialized metabolites, such as *Pseudomonas*, *Paenibacillus* and *Streptomyces*. A significant majority of these constitutive antibiotic producers were isolated from soil, suggesting that antibiotic production may not contribute to fitness in the phyllosphere. However, constitutive antibiotic producers do not represent the full metabolic capacity of either the phyllosphere or soil microbial communities. A large complement of strains either induce or produce inhibitory metabolites against *S. aureus* or *A. baumannii* only when co-cultured with another isolate. Co-cultures of phyllosphere isolates were significantly less likely than co-cultures of soil isolates to inhibit the growth of *A. baumannii* (Table 2). Because only one isolate inhibited the growth of *A. baumannii* in single culture, it is difficult to draw robust conclusions about the strategies of phyllosphere vs. soil isolates regarding antibiotic production against this organism. However, there was no difference in the proportion of interactions resulting in growth inhibition of *S. aureus* when comparing sympatric phyllosphere to soil co-cultures

(Table 2). This is in contrast with the fact that soil isolates showed a clear edge for the production of inhibitory metabolites over phyllosphere isolates in monoculture. Together, these results suggest that strategies governing antibiotic production differ in phyllosphere vs. soil communities. This is further supported by the observation that some taxa which were almost exclusively isolated from the phyllosphere (e.g. *Spingobacteriaceae*, including *Pedobacter* species), induced inhibitory compound production in co-cultures with all the major taxa responsible for antibiotic production (e.g. *Pseudomonas*, *Paenibacillus* and *Micrococcaceae*) (Figure 3 and figure S6). These results highlight the potential of phyllosphere isolates for selectively inducing antibiotic production, as well as the role of *Pedobacter* species in antagonistic interactions in plant-associated communities (Garbeva and de Boer, 2009; Garbeva, Silby, *et al.*, 2011; Tyc *et al.*, 2014). Because production of antibiotics may come at high metabolic cost (Aguirre-von-Wobeser *et al.*, 2015; Granato *et al.*, 2019), it is tempting to speculate that under oligotrophic conditions such as in the phyllosphere, facultative antibiotic production may be a favored strategy to maintain competitiveness (Garbeva, Tyc, *et al.*, 2011). The possible scenarios known to induce cryptic specialized metabolism in response to co-culturing include specific signals produced by an inducing strain to the antibiotic producer, synergistic effects of metabolites or complex metabolic interactions outside of binary chemical warfare (Zhang and Straight, 2019). Because our assay used a third strain as a read-out for antibiotic activity, we cannot reliably estimate which strain in a pair is responsible for the production of the inhibitory molecules, or which is responsible for the induction of the metabolism. We can only speculate as to the mechanisms underlying the specific induction of inhibitory activities in phyllosphere or soil isolates of our collection. Similarly, growth medium and especially carbon source, or the supplementation with sub-inhibitory concentration of antibiotics influence the production of specialized metabolites in a wide array of bacterial strains and species (Sánchez *et al.*, 2010; Seyedsayamdost, 2014). Because our screen used a single combination of growth medium and conditions, it is possible that only a small part of the potential metabolic diversity of our collection was uncovered. Understanding if, and how, the ecology of bacteria governs the mechanisms responsible for the induction of BGCs in co-cultures would undoubtedly be very valuable for guiding metabolite-mining strategies.

Intriguingly, co-culturing also often suppressed antibiotic production in strains otherwise capable of inhibiting the growth of *S. aureus* in single culture. In contrast to interactions resulting in the induction of antibiotic production, suppressive interactions were neither rare, nor specific: bacteria lost their ability to inhibit the growth of *S. aureus* while in co-culture with multiple, unrelated strains (Figure S7). Several reasons may explain this observation. Mutual growth inhibition may prevent the accumulation of metabolites in the medium to a level sufficient to inhibit the growth of *S. aureus*. Alternatively, enzymatic degradation or modification could also result in inactivation of specialized

metabolites (Wright, 2005). The apparent prevalence of this suppressive or “masking” effect in co-culture has the potential to hamper the discovery of novel molecules in screens based on bi- or multi-partite interactions. Interestingly, our data show that co-cultures of isolates from different sources (e.g. phyllosphere-soil) are significantly less likely to suppress antibiotic production than isolates from the same source (e.g. soil-soil). This indicates a degree of specificity of countermeasures to antibiosis within bacterial communities. Whether this affects the assembly and structure of plant-associated microbial communities is an open question, but this observation suggests that co-culturing of bacteria from distinct sources may be an efficient strategy to increase the likelihood of specialized metabolism induction.

Isolates which produce inhibitory metabolites in monoculture belong to taxa traditionally associated with antibiotic production such as *Pseudomonas* and *Streptomyces* (Cragg & Newman, 2013; Depoorter *et al.*, 2016). However, because antibiotic production is mostly contingent on specific signals and cues in the phyllosphere, these communities may still contain significant underexplored metabolic diversity involving taxa less commonly associated with specialized metabolite biosynthesis. We selected a pair of isolates from the phyllosphere, which produced inhibitory metabolites against the gram-negative pathogen *A. baumannii* only when cultured together. Both of these isolates represented potential novel species of *Paenibacillus* and *Sphingomonas*, which are less commonly associated with antibiotic production. We isolated acyloin metabolites from a co-culture, which show specific growth inhibitory activity against strains of the nosocomial pathogen *A. baumannii*. Indole containing xenocylins and the phenyl containing satabacins have been shown to be bioactive in the laboratory. For example, xenocylins were active against the fungi *Cryptococcus neoformans*, *Botrytis cinerea* and *Phytophthora infestans* (Paul *et al.*, 1981; Li *et al.*, 1995) and satabacins isolated from *Clostridium* were active against *S. aureus* or *Mycobacterium vaccae* (Schieferdecker *et al.*, 2019). Interestingly, satabacins showed antiviral activity against *Herpes simplex virus* (Lampis *et al.*, 1995). However, activity against *A. baumannii* is here reported for the first time for a molecule from this compound class, validating the mining of microbe-microbe interactions in under-represented environments for the discovery of natural products of clinical relevance. We also isolated the phenyl-containing acyloin compound **1** (2S,4S)-2-hydroxy-4-methyl-1-phenylhexan-3-one from a natural source for the first time and show promising antimicrobial activity against *A. baumannii* grown on solid media. Interestingly, the 2R,4R and 2R,4S isomers have recently been identified as aggregation pheromones of the velvet longhorned beetle (Ray *et al.*, 2019). It is unclear if the 2S,4S isomer, produced synthetically in the latter study, also acted as an insect pheromone. The activities reported here are above the MICs of commonly used antibiotics, with MIC breakpoints for a majority of treatment options for *A. baumannii* infections <32 mg/L (Andrews and Howe, 2011). We cannot rule

out that part or all of the antimicrobial activity of the acyloin compounds isolated here is due to the presence of undetected metabolites in our extracts. However, the specificity against *A. baumannii* and the previously described antimicrobial activity of compounds of the satabacin and xenocloin families against clinically-relevant pathogens highlights the potential of this chemical family for novel ways to treat recalcitrant infections. Our observations confirm that microbe co-culturing is a valuable strategy to widen the discovery space for novel metabolites and activities in underexplored microbial habitats.

Acknowledgements

The authors wish to thank Wim Nerinckx for the suggestions and assistance on the extraction of the potential antimicrobial compounds. We also thank Dominique Van Der Straeten for providing the seeds of *A. thaliana* for this study. This work was supported by Special Research fund of Ghent University under grant BOF17/STA/024 (to AC). AC also acknowledges support from the French Laboratory of Excellence project "TULIP" (ANR-10-LABX-41; ANR-11-IDEX-0002-02). PV wishes to acknowledge funding by the Geconcerteerde Onderzoeksacties (GOA) of Ghent University (grant BOF15/GOA/006). The Oxford Genomics Centre at the Wellcome Centre for Human Genetics is funded by Wellcome Trust grant reference 203141/Z/16/Z. The funders had no role in study design, data collection and analysis, decision to publish, or preparation of the manuscript. We thank the Oxford Genomics Centre at the Wellcome Centre for Human Genetics (funded by Wellcome Trust grant reference 203141/Z/16/Z) for the generation and initial processing of the sequencing data.

Notes

The authors declare no conflict of interest.

REFERENCES

- Abrudan, M.I., Smakman, F., Grimbergen, A.J., Westhoff, S., Miller, E.L., Van Wezel, G.P., and Rozen, D.E. (2015) Socially mediated induction and suppression of antibiosis during bacterial coexistence. *Proc Natl Acad Sci U S A* **112**: 11054–11059.
- Agler, M.T., Ruhe, J., Kroll, S., Morhenn, C., Kim, S.-T., Weigel, D., and Kemen, E.M. (2016) Microbial Hub Taxa Link Host and Abiotic Factors to Plant Microbiome Variation. *PLOS Biol* **14**: e1002352.
- Aguirre-von-Wobeser, E., Eguiarte, L.E., Souza, V., and Soberon-Chavez, G. (2015) Theoretical analysis of the cost of antagonistic activity for aquatic bacteria in oligotrophic environments. *Front Microbiol* **6**: 490.
- Alderman, D. and Smith, P. (2001) Development of draft protocols of standard reference methods for antimicrobial agent susceptibility testing of bacteria associated with fish diseases.

Aquaculture **196**: 211–243.

- Altschul, S.F., Gish, W., Miller, W., Myers, E.W., and Lipman, D.J. (1990) Basic local alignment search tool. *J Mol Biol* **215**: 403–10.
- Andrews, J.M. and Howe, R.A. (2011) BSAC standardized disc susceptibility testing method (version 10). *J Antimicrob Chemother* **66**: 2726–2757.
- Aronoff, M.R., Bourjaily, N.A., and Miller, K.A. (2010) Concise, protecting group free total syntheses of (+)-sattabacin and (+)-4-hydroxysattabacin. *Tetrahedron Lett* **51**: 6375–6377.
- Bai, Y., Müller, D.B., Srinivas, G., Garrido-Oter, R., Potthoff, E., Rott, M., et al. (2015) Functional overlap of the Arabidopsis leaf and root microbiota. *Nature* **528**: 364–369.
- Bangera, G.M. (1996) Characterization of a Genomic Locus Required for Synthesis of the Antibiotic 2,4-diacetylphloroglucinol by the Biological Control Agent *Pseudomonas fluorescens* Q2-87. *Mol Plant-Microbe Interact* **9**: 083.
- Bankevich, A., Nurk, S., Antipov, D., Gurevich, A.A., Dvorkin, M., Kulikov, A.S., et al. (2012) SPAdes: a new genome assembly algorithm and its applications to single-cell sequencing. *J Comput Biol* **19**: 455–77.
- Barberán, A., Bates, S.T., Casamayor, E.O., and Fierer, N. (2012) Using network analysis to explore co-occurrence patterns in soil microbial communities. *ISME J* **6**: 343–351.
- Blair, P.M., Land, M.L., Piatek, M.J., Jacobson, D.A., Lu, T.-Y.S., Doktycz, M.J., and Pelletier, D.A. (2018) Exploration of the Biosynthetic Potential of the Populus Microbiome. *mSystems* **3**.
- Blin, K., Shaw, S., Steinke, K., Villebro, R., Ziemert, N., Lee, S.Y., et al. (2019) antiSMASH 5.0: updates to the secondary metabolite genome mining pipeline. *Nucleic Acids Res* **47**: W81–W87.
- Bodenhausen, N., Horton, M.W., and Bergelson, J. (2013) Bacterial Communities Associated with the Leaves and the Roots of *Arabidopsis thaliana*. *PLoS One* **8**: e56329.
- Bolger, A.M., Lohse, M., and Usadel, B. (2014) Trimmomatic: a flexible trimmer for Illumina sequence data. *Bioinformatics* **30**: 2114–20.
- Bolyen, E., Rideout, J.R., Dillon, M.R., Bokulich, N.A., Abnet, C., Al-Ghalith, G.A., et al. (2018) QIIME 2: Reproducible, interactive, scalable, and extensible microbiome data science.
- Bulgarelli, D., Schlaeppli, K., Spaepen, S., Ver Loren van Themaat, E., and Schulze-Lefert, P. (2013) Structure and functions of the bacterial microbiota of plants. *Annu Rev Plant Biol* **64**: 807–38.
- Callahan, B.J., McMurdie, P.J., Rosen, M.J., Han, A.W., Johnson, A.J.A., and Holmes, S.P. (2016) DADA2: High-resolution sample inference from Illumina amplicon data. *Nat Methods* **13**: 581–583.
- Capella-Gutiérrez, S., Silla-Martínez, J.M., and Gabaldón, T. (2009) trimAl: a tool for automated alignment trimming in large-scale phylogenetic analyses. *Bioinformatics* **25**: 1972–3.
- Carlier, A., Fehr, L., Pinto-Carbó, M., Schäberle, T., Reher, R., Dessen, S., et al. (2016) The genome analysis of *Candidatus Burkholderia crenata* reveals that secondary metabolism may be a key function of the *Ardisia crenata* leaf nodule symbiosis. *Environ Microbiol* **18**: 2507–2522.
- Carrión, V.J., Perez-Jaramillo, J., Cordovez, V., Tracanna, V., de Hollander, M., Ruiz-Buck, D., et al. (2019) Pathogen-induced activation of disease-suppressive functions in the endophytic root microbiome. *Science (80-)* **366**: 606–612.
- CDC (2019) Antibiotic resistance threats in the United States, 2019, Atlanta, Georgia.

- Chaffron, S., Rehrauer, H., Pernthaler, J., and von Mering, C. (2010) A global network of coexisting microbes from environmental and whole-genome sequence data. *Genome Res* **20**: 947–959.
- Chen, T., Nomura, K., Wang, X., Sohrabi, R., Xu, J., Yao, L., et al. (2020) A plant genetic network for preventing dysbiosis in the phyllosphere. *Nature* **580**: 653–657.
- Copeland, J.K., Yuan, L., Layeghifard, M., Wang, P.W., and Guttman, D.S. (2015) Seasonal community succession of the phyllosphere microbiome. *Mol Plant-Microbe Interact* **28**: 274–285.
- Cordero, O.X. and Datta, M.S. (2016) Microbial interactions and community assembly at microscales. *Curr Opin Microbiol* **31**: 227–234.
- Cornforth, D.M. and Foster, K.R. (2013) Competition sensing: The social side of bacterial stress responses. *Nat Rev Microbiol* **11**: 285–293.
- Cragg, G.M. and Newman, D.J. (2013) Natural products: A continuing source of novel drug leads. *Biochim Biophys Acta - Gen Subj* **1830**: 3670–3695.
- Crits-Christoph, A., Diamond, S., Butterfield, C.N., Thomas, B.C., and Banfield, J.F. (2018) Novel soil bacteria possess diverse genes for secondary metabolite biosynthesis. *Nature* **558**: 440–444.
- Cuesta, G., García-de-la-Fuente, R., Abad, M., and Fornes, F. (2012) Isolation and identification of actinomycetes from a compost-amended soil with potential as biocontrol agents. *J Environ Manage* **95**: S280–S284.
- Dandurishvili, N., Toklikishvili, N., Ovadis, M., Eliashvili, P., Giorgobiani, N., Keshelava, R., et al. (2011) Broad-range antagonistic rhizobacteria *Pseudomonas fluorescens* and *Serratia plymuthica* suppress *Agrobacterium* crown gall tumours on tomato plants. *J Appl Microbiol* **110**: 341–352.
- Depoorter, E., Bull, M.J., Peeters, C., Coenye, T., Vandamme, P., and Mahenthiralingam, E. (2016) Burkholderia: an update on taxonomy and biotechnological potential as antibiotic producers. *Appl Microbiol Biotechnol* **100**: 5215–5229.
- Dijkshoorn, L., Aucken, H., Gerner-Smidt, P., Janssen, P., Kaufmann, M.E., Garaizar, J., et al. (1996) Comparison of outbreak and nonoutbreak *Acinetobacter baumannii* strains by genotypic and phenotypic methods. *J Clin Microbiol* **34**: 1519–1525.
- Dumolin, C., Aerts, M., Verheyde, B., Schellaert, S., Vandamme, T., Van der Jeugt, F., et al. (2019) Introducing SPeDE: High-Throughput Dereplication and Accurate Determination of Microbial Diversity from Matrix-Assisted Laser Desorption–Ionization Time of Flight Mass Spectrometry Data. *mSystems* **4**:
- Faust, K. and Raes, J. (2012) Microbial interactions: from networks to models. *Nat Rev Microbiol* **10**: 538–550.
- Faust, K., Sathirapongsasuti, J.F., Izard, J., Segata, N., Gevers, D., Raes, J., and Huttenhower, C. (2012) Microbial Co-occurrence Relationships in the Human Microbiome. *PLoS Comput Biol* **8**: e1002606.
- Firn, R.D. and Jones, C.G. (2003) Natural products ? a simple model to explain chemical diversity. *Nat Prod Rep* **20**: 382.
- Ganley, J.G., Carr, G., Ioerger, T.R., Sacchetti, J.C., Clardy, J., and Derbyshire, E.R. (2018) Discovery of Antimicrobial Lipopeptides Produced by a *Serratia* sp. within Mosquito Microbiomes. *ChemBioChem* **19**: 1590–1594.
- Garbeva, P. and de Boer, W. (2009) Inter-specific Interactions Between Carbon-limited Soil Bacteria Affect Behavior and Gene Expression. *Microb Ecol* **58**: 36–46.

- Accepted Article
- Garbeva, P., Silby, M.W., Raaijmakers, J.M., Levy, S.B., and Boer, W. de (2011) Transcriptional and antagonistic responses of *Pseudomonas fluorescens* Pf0-1 to phylogenetically different bacterial competitors. *ISME J* **5**: 973–985.
- Garbeva, P., Tyc, O., Remus-Emsermann, M.N.P., van der Wal, A., Vos, M., Silby, M., and de Boer, W. (2011) No apparent costs for facultative antibiotic production by the soil bacterium *Pseudomonas fluorescens* Pf0-1. *PLoS One* **6**:
- Granato, E.T., Meiller-Legrand, T.A., and Foster, K.R. (2019) The Evolution and Ecology of Bacterial Warfare. *Curr Biol* **29**: R521–R537.
- Grubbs, K.J., Bleich, R.M., Santa Maria, K.C., Allen, S.E., Farag, S., Shank, E.A., and Bowers, A.A. (2017) Large-Scale Bioinformatics Analysis of *Bacillus* Genomes Uncovers Conserved Roles of Natural Products in Bacterial Physiology. *mSystems* **2**:
- Guidi, L., Chaffron, S., Bittner, L., Eveillard, D., Larhlimi, A., Roux, S., et al. (2016) Plankton networks driving carbon export in the oligotrophic ocean. *Nature* **532**: 465–470.
- Helfrich, E.J.N.N., Vogel, C.M., Ueoka, R., Schäfer, M., Ryffel, F., Müller, D.B., et al. (2018) Bipartite interactions, antibiotic production and biosynthetic potential of the *Arabidopsis* leaf microbiome. *Nat Microbiol* **3**: 909–919.
- Hibbing, M.E., Fuqua, C., Parsek, M.R., and Peterson, S.B. (2010) Bacterial competition: surviving and thriving in the microbial jungle. *Nat Rev Microbiol* **8**: 15–25.
- Hsiao, C.-C., Sieber, S., Georgiou, A., Bailly, A., Emmanouilidou, D., Carlier, A., et al. (2019) Synthesis and Biological Evaluation of the Novel Growth Inhibitor Streptol Glucoside, Isolated from an Obligate Plant Symbiont. *Chem - A Eur J* **25**: 1722–1726.
- Hunter, P.J., Hand, P., Pink, D., Whipps, J.M., and Bending, G.D. (2010) Both leaf properties and microbe-microbe interactions influence within-species variation in bacterial population diversity and structure in the lettuce (*Lactuca* species) phyllosphere. *Appl Environ Microbiol* **76**: 8117–8125.
- Huys, G., Cnockaert, M., Vanechoutte, M., Woodford, N., Nemec, A., Dijkshoorn, L., and Swings, J. (2005) Distribution of tetracycline resistance genes in genotypically related and unrelated multiresistant *Acinetobacter baumannii* strains from different European hospitals. *Res Microbiol* **156**: 348–355.
- Imai, Y., Meyer, K.J., Iinishi, A., Favre-Godal, Q., Green, R., Manuse, S., et al. (2019) A new antibiotic selectively kills Gram-negative pathogens. *Nature* **576**: 459–464.
- Janssen, P., Maquelin, K., Coopman, R., Tjernberg, I., Bouvet, P., Kersters, K., and Dijkshoorn, L. (1997) Discrimination of *Acinetobacter* Genomic Species by AFLP Fingerprinting. *Int J Syst Bacteriol* **47**: 1179–1187.
- Jiang, L., Pu, H., Qin, X., Liu, J., Wen, Z., Huang, Yimin, et al. (2019) Syn-2, 3-diols and anti-inflammatory indole derivatives from *Streptomyces* sp. CB09001. *Nat Prod Res* 1–8.
- Katoh, K. and Standley, D.M. (2013) MAFFT multiple sequence alignment software version 7: improvements in performance and usability. *Mol Biol Evol* **30**: 772–80.
- Kinkel, L.L. (1997) Microbial Population Dynamics on Leaves. *Annu Rev Phytopathol* **35**: 327–347.
- Knief, C., Delmotte, N., Chaffron, S., Stark, M., Innerebner, G., Wassmann, R., et al. (2012) Metaproteogenomic analysis of microbial communities in the phyllosphere and rhizosphere of rice. *ISME J* **6**: 1378–90.

- Kurtz, Z.D., Müller, C.L., Miraldi, E.R., Littman, D.R., Blaser, M.J., and Bonneau, R.A. (2015) Sparse and Compositionally Robust Inference of Microbial Ecological Networks. *PLOS Comput Biol* **11**: e1004226.
- Lampis, G., Deidda, D., Maullu, C., Madeddu, M.A., Pompei, R., Delle Monachie, F., and Satta, G. (1995) Sattabacins and sattazolins: new biologically active compounds with antiviral properties extracted from a *Bacillus* sp. *J Antibiot (Tokyo)* **48**: 967–72.
- Leveau, J.H.J. and Lindow, S.E. (2001) Appetite of an epiphyte: Quantitative monitoring of bacterial sugar consumption in the phyllosphere. *Proc Natl Acad Sci* **98**: 3446–3453.
- Levy, A., Salas Gonzalez, I., Mittelviehhaus, M., Clingenpeel, S., Herrera Paredes, S., Miao, J., et al. (2018) Genomic features of bacterial adaptation to plants. *Nat Genet* **50**: 138–150.
- Li, J., Chen, G., Webster, J.M., Czyzewska, E., and Czyzewska, E. (1995) Antimicrobial Metabolites from a Bacterial Symbiont. *J Nat Prod* **58**: 1081–1086.
- Lindow, S.E. and Brandl, M.T. (2003) Microbiology of the phyllosphere. *Appl Environ Microbiol* **69**: 1875–83.
- Ling, L.L., Schneider, T., Peoples, A.J., Spoering, A.L., Engels, I., Conlon, B.P., et al. (2015) A new antibiotic kills pathogens without detectable resistance. *Nature* **517**: 455–459.
- Lu, C. and Shen, Y. (2003) A New Macrolide Antibiotic with Antitumor Activity Produced by *Streptomyces* sp. CS, a Commensal Microbe of *Maytenus hookeri*. *J Antibiot (Tokyo)* **56**: 415–418.
- Ma, B., Wang, H., Dsouza, M., Lou, J., He, Y., Dai, Z., et al. (2016) Geographic patterns of co-occurrence network topological features for soil microbiota at continental scale in eastern China. *ISME J* **10**: 1891–1901.
- Mahenthiralingam, E., Song, L., Sass, A., White, J., Wilmot, C., Marchbank, A., et al. (2011) Enacyloxins Are Products of an Unusual Hybrid Modular Polyketide Synthase Encoded by a Cryptic *Burkholderia ambifaria* Genomic Island. *Chem Biol* **18**: 665–677.
- Maignien, L., DeForce, E.A., Chafee, M.E., Murat Eren, A., and Simmons, S.L. (2014) Ecological succession and stochastic variation in the assembly of *Arabidopsis thaliana* phyllosphere communities. *MBio* **5**:
- Marçais, G. and Kingsford, C. (2011) A fast, lock-free approach for efficient parallel counting of occurrences of k-mers. *Bioinformatics* **27**: 764–770.
- Massoni, J., Bortfeld-Miller, M., Jardillier, L., Salazar, G., Sunagawa, S., and Vorholt, J.A. (2019) Consistent host and organ occupancy of phyllosphere bacteria in a community of wild herbaceous plant species. *ISME J*.
- McMurdie, P.J. and Holmes, S. (2013) phyloseq: An R Package for Reproducible Interactive Analysis and Graphics of Microbiome Census Data. *PLoS One* **8**: e61217.
- De Meyer, F., Danneels, B., Acar, T., Rasolomampianina, R., Rajaonah, M.T., Jeannoda, V., and Carlier, A. (2019) Adaptations and evolution of a heritable leaf nodule symbiosis between *Dioscorea sansibarensis* and *Orrella dioscoreae*. *ISME J* **13**: 1831–1844.
- Miller, W.G., Brandl, M.T., Quiñones, B., and Lindow, S.E. (2001) Biological Sensor for Sucrose Availability: Relative Sensitivities of Various Reporter Genes. *Appl Environ Microbiol* **67**: 1308–1317.
- Mukherjee, S., Seshadri, R., Varghese, N.J., Eloë-Fadrosh, E.A., Meier-Kolthoff, J.P., Göker, M., et al.

(2017) 1,003 reference genomes of bacterial and archaeal isolates expand coverage of the tree of life. *Nat Biotechnol* **35**: 676–683.

- Nemec, A., Dolzani, L., Brisse, S., Van Den Broek, P., and Dijkshoorn, L. (2004) Diversity of aminoglycoside-resistance genes and their association with class 1 integrons among strains of pan-European *Acinetobacter baumannii* clones. *J Med Microbiol* **53**: 1233–1240.
- Newman, D.J. and Cragg, G.M. (2020) Natural Products as Sources of New Drugs over the Nearly Four Decades from 01/1981 to 09/2019. *J Nat Prod* **83**: 770–803.
- Niemann, S., Pühler, A., Tichy, H. -V., Simon, R., and Selbitschka, W. (1997) Evaluation of the resolving power of three different DNA fingerprinting methods to discriminate among isolates of a natural *Rhizobium meliloti* population. *J Appl Microbiol* **82**: 477–484.
- O’Neill, J. (2014) Review on Antimicrobial Resistance. Antimicrobial Resistance: Tackling a Crisis for the Health and Wealth of Nations.
- Park, J.-S., Kagaya, N., Hashimoto, J., Izumikawa, M., Yabe, S., Shin-ya, K., et al. (2014) Identification and Biosynthesis of New Acyloins from the Thermophilic Bacterium *Thermosporothrix hazakensis* SK20 - 1 T. *ChemBioChem* **15**: 527–532.
- Paul, V.J., Frautschy, S., Fenical, W., and Neelson, K.H. (1981) ANTIBIOTICS IN MICROBIAL ECOLOGY Isolation and Structure Assignment of Several New Antibacterial Compounds from the Insect-Symbiotic Bacteria *Xenorhabdus* spp.
- Peeters, C., Depoorter, E., Praet, J., and Vandamme, P. (2016) Extensive cultivation of soil and water samples yields various pathogens in patients with cystic fibrosis but not *Burkholderia multivorans*. *J Cyst Fibros* **15**: 769–775.
- Pendleton, J.N., Gorman, S.P., and Gilmore, B.F. (2013) Clinical relevance of the ESKAPE pathogens. *Expert Rev Anti Infect Ther* **11**: 297–308.
- Pinto-Carbó, M., Gademann, K., Eberl, L., and Carlier, A. (2018) Leaf nodule symbiosis: function and transmission of obligate bacterial endophytes. *Curr Opin Plant Biol* **44**: 23–31.
- Pinto-Carbó, M., Sieber, S., Dessein, S., Wicker, T., Verstraete, B., Gademann, K., et al. (2016) Evidence of horizontal gene transfer between obligate leaf nodule symbionts. *ISME J* **10**: 2092–2105.
- Price, M.N., Dehal, P.S., and Arkin, A.P. (2010) FastTree 2 – Approximately Maximum-Likelihood Trees for Large Alignments. *PLoS One* **5**: e9490.
- Proschak, A., Zhou, Q., Schöner, T., Thanwisai, A., Kresovic, D., Dowling, A., et al. (2014) Biosynthesis of the insecticidal xenoclyloins in *xenorhabdus bovienii*. *ChemBioChem* **15**: 369–372.
- Quast, C., Pruesse, E., Yilmaz, P., Gerken, J., Schweer, T., Yarza, P., et al. (2013) The SILVA ribosomal RNA gene database project: improved data processing and web-based tools. *Nucleic Acids Res* **41**: D590-6.
- R Core Team (2014) R: A Language and Environment for Statistical Computing.
- Rainey, F.A. (2015) Clostridiales. In *Bergey’s Manual of Systematics of Archaea and Bacteria*. Chichester, UK: John Wiley & Sons, Ltd, pp. 1–5.
- Ray, A.M., Francese, J.A., Zou, Y., Watson, K., Crook, D.J., and Millar, J.G. (2019) Isolation and identification of a male-produced aggregation-sex pheromone for the velvet longhorned beetle, *Trichoferus campestris*. *Sci Rep* **9**: 4459.
- Remus-Emsermann, M.N.P., Lückner, S., Müller, D.B., Potthoff, E., Daims, H., and Vorholt, J.A. (2014)

Spatial distribution analyses of natural phyllosphere-colonizing bacteria on *A. radicans* revealed by fluorescence in situ hybridization. *Environ Microbiol* **16**: 2329–2340.

- Remus-Emsermann, M.N.P., Tecon, R., Kowalchuk, G.A., and Leveau, J.H.J. (2012) Variation in local carrying capacity and the individual fate of bacterial colonizers in the phyllosphere. *ISME J* **6**: 756–765.
- Sánchez, S., Chávez, A., Forero, A., García-Huante, Y., Romero, A., Sánchez, M., et al. (2010) Carbon source regulation of antibiotic production. *J Antibiot (Tokyo)* **63**: 442–459.
- Scherlach, K. and Hertweck, C. (2009) Triggering cryptic natural product biosynthesis in microorganisms. *Org Biomol Chem* **7**: 1753.
- Schieferdecker, S., Shabuer, G., Letzel, A.-C., Urbansky, B., Ishida-Ito, M., Ishida, K., et al. (2019) Biosynthesis of Diverse Antimicrobial and Antiproliferative Acyloins in Anaerobic Bacteria. *ACS Chem Biol* **14**: 1490–1497.
- Schlechter, R.O., Miebach, M., and Remus-Emsermann, M.N.P. (2019) Driving factors of epiphytic bacterial communities: A review. *J Adv Res* **19**: 57–65.
- Schroeckh, V., Scherlach, K., Nutzmann, H.-W., Shelest, E., Schmidt-Heck, W., Schuemann, J., et al. (2009) Intimate bacterial-fungal interaction triggers biosynthesis of archetypal polyketides in *Aspergillus nidulans*. *Proc Natl Acad Sci* **106**: 14558–14563.
- Seyedsayamdost, M.R. (2014) High-Throughput platform for the discovery of elicitors of silent bacterial gene clusters. *Proc Natl Acad Sci U S A* **111**: 7266–7271.
- Seyedsayamdost, M.R., Traxler, M.F., Clardy, J., and Kolter, R. (2012) Old meets new: Using interspecies interactions to detect secondary metabolite production in actinomycetes. In *Methods in Enzymology*. Academic Press Inc., pp. 89–109.
- Sieber, S., Carlier, A., Neuburger, M., Grabenweger, G., Eberl, L., and Gademann, K. (2015) Isolation and Total Synthesis of Kirkamide, an Aminocyclitol from an Obligate Leaf Nodule Symbiont. *Angew Chemie Int Ed* **54**: 7968–7970.
- Soni, I., Chakrapani, H., and Chopra, S. (2015) Draft Genome Sequence of Methicillin-Sensitive *Staphylococcus aureus* ATCC 29213. *Genome Announc* **3**:
- Souvorov, A., Agarwala, R., and Lipman, D.J. (2018) SKESA: strategic k-mer extension for scrupulous assemblies. *Genome Biol* **19**: 153.
- Tacconelli, E., Carrara, E., Savoldi, A., Harbarth, S., Mendelson, M., Monnet, D.L., et al. (2018) Discovery, research, and development of new antibiotics: the WHO priority list of antibiotic-resistant bacteria and tuberculosis. *Lancet Infect Dis* **18**: 318–327.
- Tkacz, A., Bestion, E., Bo, Z., Hortalá, M., and Poole, P.S. (2020) Influence of Plant Fraction, Soil, and Plant Species on Microbiota: a Multikingdom Comparison. *MBio* **11**:
- Turton, J.F., Kaufmann, M.E., Gill, M.J., Pike, R., Scott, P.T., Fishbain, J., et al. (2006) Comparison of *Acinetobacter baumannii* Isolates from the United Kingdom and the United States That Were Associated with Repatriated Casualties of the Iraq Conflict. *J Clin Microbiol* **44**: 2630–2634.
- Tyc, O., van den Berg, M., Gerards, S., van Veen, J.A., Raaijmakers, J.M., de Boer, W., and Garbeva, P. (2014) Impact of interspecific interactions on antimicrobial activity among soil bacteria. *Front Microbiol* **5**: 567.
- Ueoka, R., Meoded, R.A., Gran-Scheuch, A., Bhushan, A., Fraaije, M.W., and Piel, J. (2020) Genome Mining of Oxidation Modules in trans -Acyltransferase Polyketide Synthases Reveals a

Culturable Source for Lobatamides. *Angew Chemie Int Ed* **59**: 7761–7765.

Vorholt, J.A. (2012) Microbial life in the phyllosphere. *Nat Rev Microbiol* **10**: 828–40.

Whipps, J.M., Hand, P., Pink, D., and Bending, G.D. (2008) Phyllosphere microbiology with special reference to diversity and plant genotype. *J Appl Microbiol* **105**: 1744–1755.

Wilson, K. (2001) Preparation of Genomic DNA from Bacteria, John Wiley & Sons, Inc.

Wright, G.D. (2005) Bacterial resistance to antibiotics: Enzymatic degradation and modification. *Adv Drug Deliv Rev* **57**: 1451–1470.

Yadav, R.K.P., Papatheodorou, E.M., Karamanoli, K., Constantinidou, H.I.A., and Vokou, D. (2008) Abundance and diversity of the phyllosphere bacterial communities of Mediterranean perennial plants that differ in leaf chemistry. *Chemoecology* **18**: 217–226.

Zhang, C. and Straight, P.D. (2019) Antibiotic discovery through microbial interactions. *Curr Opin Microbiol* **51**: 64–71.

Zhu, S., Hegemann, J.D., Fage, C.D., Zimmermann, M., Xie, X., Linne, U., and Marahiel, M.A. (2016) Insights into the Unique Phosphorylation of the Lasso Peptide Paeninodin. *J Biol Chem* **291**: 13662–13678.

Zipperer, A., Konnerth, M.C., Laux, C., Berscheid, A., Janek, D., Weidenmaier, C., et al. (2016) Human commensals producing a novel antibiotic impair pathogen colonization. *Nature* **535**: 511–516.

Legends:

Figure 1: Experimental design. This experiment was carried out in closed, autoclaved tissue culture containers, filled with twice-autoclaved pumice stones and half-strength MS-medium. Containers were sown with surface-sterilized seeds of *Arabidopsis thaliana* and inoculated with a soil suspension or a mock solution (A and C, respectively). Other pots contained pumice stones inoculated with a soil suspension or a mock solution, but were left unplanted (B and D, respectively). Plants were incubated in a standard incubator for about one month, after which the samples from each of the four group were collected for the culture-independent and culture-dependent downstream analyses.

Figure 2. Most abundant taxa in the different plant compartments. The Top 100 most abundant amplicon sequencing variants (ASVs) are considered from planted soil (orange squares), unplanted soil (brown squares) and the phyllosphere (green squares). Each ASV represents a distinct variant of a V3-V4 16S rRNA gene marker sequence (see materials and methods for details). Pink circles denote ASV sequences matching near-full length 16S rRNA sequences from the isolate collection with > 99% identity. Colored ranges denote the taxonomic assignments (phylum) of the ASVs. Branches colored in red denote the Order *Clostridiales*, for which no representative was obtained in the isolation campaign. The phylogenetic tree was built using the maximum likelihood method on an alignment of ASVs.

Figure 3. Taxonomic composition and phenotypes of the culture collection. The maximum-likelihood phylogeny was constructed based on nearly full-length 16S rRNA sequences (see materials and methods). Symbols on the centermost ring denote the isolation origin of the strain: phyllosphere (green triangle), soil (brown triangle) or pumice (grey triangle). Square symbols on the outer rings show matches between partial 16S rRNA gene sequence of an isolate to a top 100 most abundant ASV obtained in culture-independent analysis of the different plant compartments (>99% sequence identity). Yellow connecting lines between each two isolates represent the active antimicrobial activity towards *S. aureus* LMG 10147, red lines indicate the active antibiotic activity against *A. baumannii* LMG 10520. Isolates capable of antibiotic production in monoculture are denoted with a blue star.

Figure 4. Network of pairwise co-cultures resulting in growth inhibitory activity. Green nodes represent isolates from the phyllosphere, brown nodes represent bacterial isolates from soil, grey nodes represent isolates from uninoculated pumice. Red lines represent interactions resulting in growth inhibition of *A. baumannii* LMG 10520, yellow lines show the inhibitory activity towards *S. aureus* LMG 10147.

Figure 5. Isolation of compounds from a co-culture of *Paenibacillus* sp. P3_m116_1 and *Sphingomonas* sp. P2_m126_1 inhibiting the growth of *A. baumannii*. A. Extracts of a co-culture were separated by vacuum liquid chromatography to yield 7 fractions, and 2 mg of each fraction were tested for growth inhibition of *A. baumannii* in an overlay assay, with fraction VLC5 displaying the clearest inhibition zones. B. Compounds 1-5 were isolated after further fractionation and activity testing. Compounds 2,3,4 and 5 have been discovered and isolated from *Xenorhabdus* spp (Proschak *et al.*, 2014), and biosynthesised recently (Park *et al.*, 2014; Schieferdecker *et al.*, 2019). Compound 1 is a new natural product active on *A. baumannii* LMG 10520. C. Putative gene cluster involved in acyloin production by *Paenibacillus* sp. P3_m116_1 (C). Genes GC101_RS07275 and show significant similarity to TPP-dependent acyloin synthases Thzk0150 of *Thermosporothrix hazakensis* and Cbei2730 of *Clostridium beijerinckii* (25% and 31% identity, respectively). Note: the picture in panel A was edited to remove markings on the Petri dish. The original is shown in Figure S9.

Table 1: List of strains producing inhibition zones in monoculture

Strain	Taxonomy	Isolation source	Test organism
P3_m158_1	<i>Pseudomonas</i> sp.	Phyllosphere	<i>S. aureus</i> LMG 10147
P2_m50_1	<i>Pseudomonas</i> sp.	Phyllosphere	<i>S. aureus</i> LMG 10147
P3_m166_1	<i>Pseudomonas</i> sp.	Phyllosphere	<i>S. aureus</i> LMG 10147
P2_m24_1	<i>Pseudomonas</i> sp.	Phyllosphere	<i>S. aureus</i> LMG 10147
P2_m30_1	<i>Pseudomonas</i> sp.	Phyllosphere	<i>S. aureus</i> LMG 10147
S2_m61_1	<i>Pseudomonas</i> sp.	Soil	<i>S. aureus</i> LMG 10147
S3_m132_1	<i>Pseudomonas</i> sp.	Soil	<i>S. aureus</i> LMG 10147
S3_m138_1	<i>Pseudomonas</i> sp.	Soil	<i>S. aureus</i> LMG 10147
S3_m201_1	<i>Pseudomonas</i> sp.	Soil	<i>S. aureus</i> LMG 10147
S3_m206_1	<i>Pseudomonas</i> sp.	Soil	<i>S. aureus</i> LMG 10147
S2_m234_1	<i>Pseudomonas</i> sp.	Soil	<i>S. aureus</i> LMG 10147
S3_m202_1	<i>Pseudomonas</i> sp.	Soil	<i>S. aureus</i> LMG 10147
S3_m207_1	<i>Streptomyces</i> sp.	Soil	<i>S. aureus</i> LMG 10147
S3_m208_1	<i>Streptomyces</i> sp.	Soil	<i>S. aureus</i> LMG 10147
P2_m90_1	<i>Pseudomonas</i> sp.	Phyllosphere	<i>S. aureus</i> LMG 10147
P2_m8_1	<i>Pseudomonas</i> sp.	Soil	<i>S. aureus</i> LMG 10147
S2_m13_1	<i>Pseudomonas</i> sp.	Soil	<i>S. aureus</i> LMG 10147
S2_m5_1	<i>Pseudomonas</i> sp.	Soil	<i>S. aureus</i> LMG 10147
S2_m9_2	<i>Pseudomonas</i> sp.	Soil	<i>S. aureus</i> LMG 10147
S2_m3_1	<i>Pseudomonas</i> sp.	Soil	<i>S. aureus</i> LMG 10147
S2_m230_1	<i>Pseudomonas</i> sp.	Soil	<i>S. aureus</i> LMG 10147
S2_m10_3	<i>Pseudomonas</i> sp.	Soil	<i>S. aureus</i> LMG 10147
P3_m182_1	<i>Paenibacillus</i> sp.	Phyllosphere	<i>S. aureus</i> LMG 10147
S2_m100_1	<i>Pseudomonas</i> sp.	Soil	<i>S. aureus</i> LMG 10147
S2_m52_1	<i>Pseudomonas</i> sp.	Soil	<i>S. aureus</i> LMG 10147
S2_m61_2	<i>Pseudomonas</i> sp.	Soil	<i>S. aureus</i> LMG 10147
P3_m122_1	<i>Staphylococcus</i> sp.	Phyllosphere	<i>A. baumannii</i> LMG 10520
S2_m11_1	<i>Pseudomonas</i> sp.	Soil	<i>S. aureus</i> LMG 10147

Table 2. Summary of the results of the bipartite interaction screen.

Co-culture	Isolate source	Overall inhibitory interactions	Inhibitory vs. <i>A. baumannii</i> LMG 10520	Inhibitory vs. <i>S. aureus</i> LMG 10147
Inhibition during bipartite interactions only	S-S	33/1496 (2.21%)	20/700 (2.85%)	13/796 (1.63%)
	P-P	78/6492 (1.20%)	28/3150 (0.89%)	50/3342 (1.96%)
	P-S	115/6671 (1.72%)	73/3216 (2.26%)	42/3455 (1.22%)
Suppressive interactions ^a	S-S	-	nd	119/420 (28.33%)
	P-P	-	nd	180/600 (30.00%)
	P-S	-	nd	268/1189 (22.53%)

S, Soil; P, Phyllosphere; nd, not determined. Number of inhibitory interactions in the overlay assay are given in the numerator, total number of combinations tested in the denominator. Percentages are given in parenthesis. ^a Suppressive interactions denote interactions involving at least 1 strain which produces inhibitory metabolites constitutively, but do not result in inhibition zones in the overlay assay. For clarity, interactions between isolates of sources other than P and S are not represented here: only 2 interactions between unplanted soil and soil isolates resulted in *S. aureus* growth inhibition.

Table 3. Minimum inhibitory concentrations (MIC) of compounds sattabacin (**2**) and xenoclyoin B (**4**) against *A. baumannii*.

Strain	Compound 2 MIC (µg/ml)	Compound 4 MIC (µg/ml)
<i>Acinetobacter baumannii</i> 70PUS	32	32
<i>Acinetobacter baumannii</i> RUH 0134	32	32
<i>Acinetobacter baumannii</i> NCTC 13423	32	32
<i>Acinetobacter baumannii</i> RUH 3247	64	32
<i>Acinetobacter baumannii</i> LUH 3788	32	32
<i>Acinetobacter baumannii</i> A1392	64	32
<i>Acinetobacter baumannii</i> LMG 10520	64	64

Table S1. Taxonomic classification of individual strains of the collection based on near full-length 16S rRNA gene sequence.

Table S2. Growth inhibition of co-cultures of pairs of isolates against *Acinetobacter baumannii* and *Staphylococcus aureus* in an overlay assay.



Autoclaved pumice



Surface sterilized
seeds developed into
plants after one
month

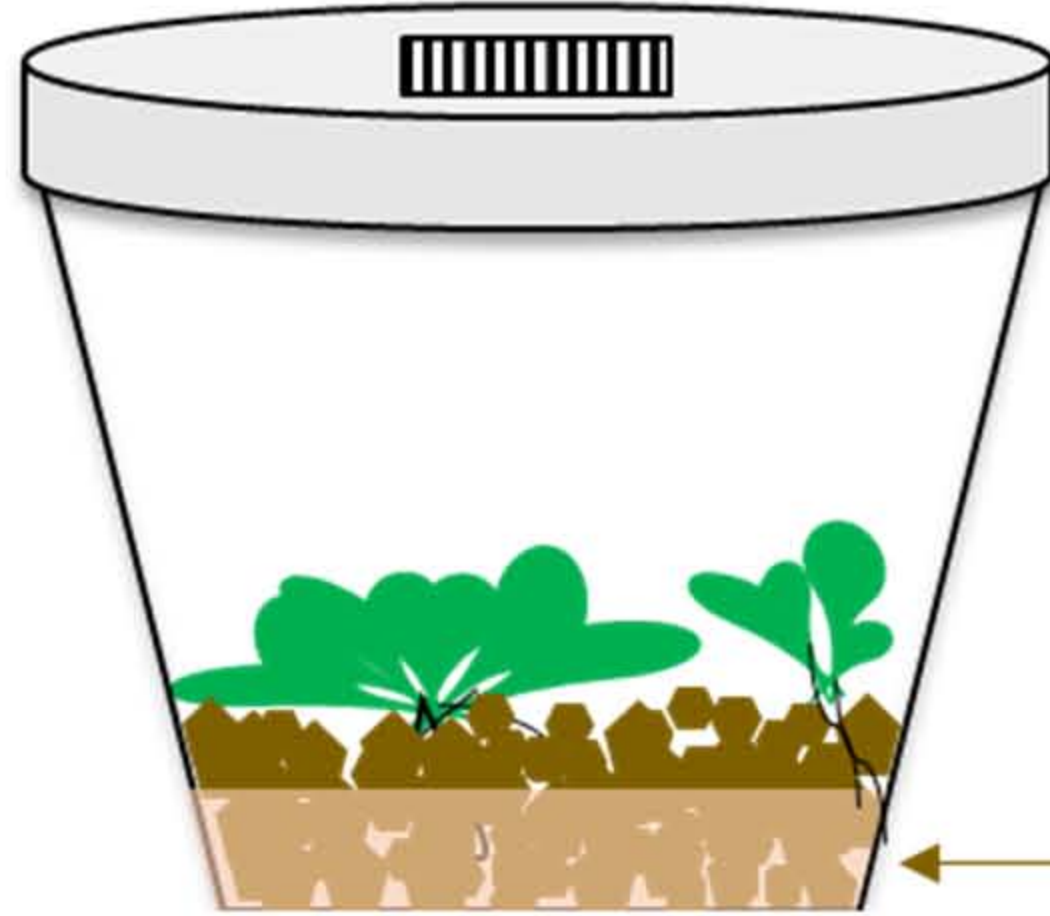


1/2 MS + soil supernatant

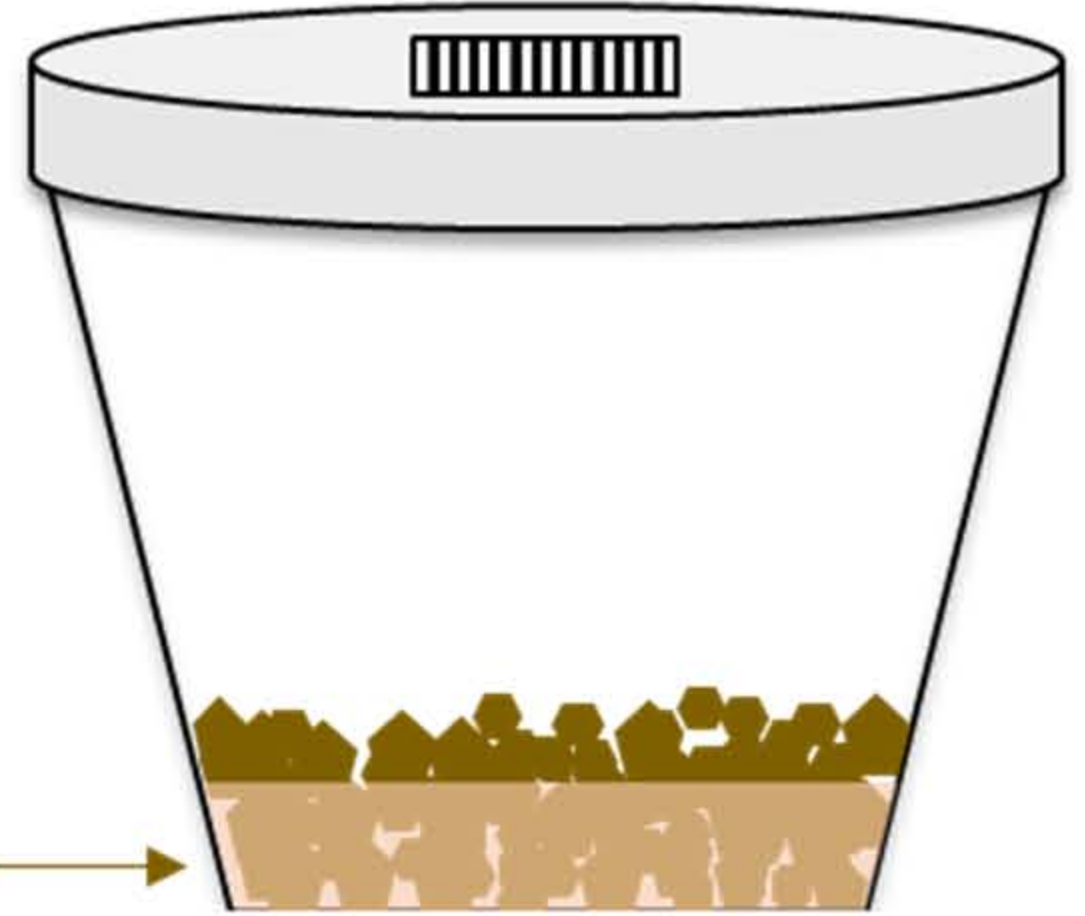


1/2 MS + 0.5xPBS

A

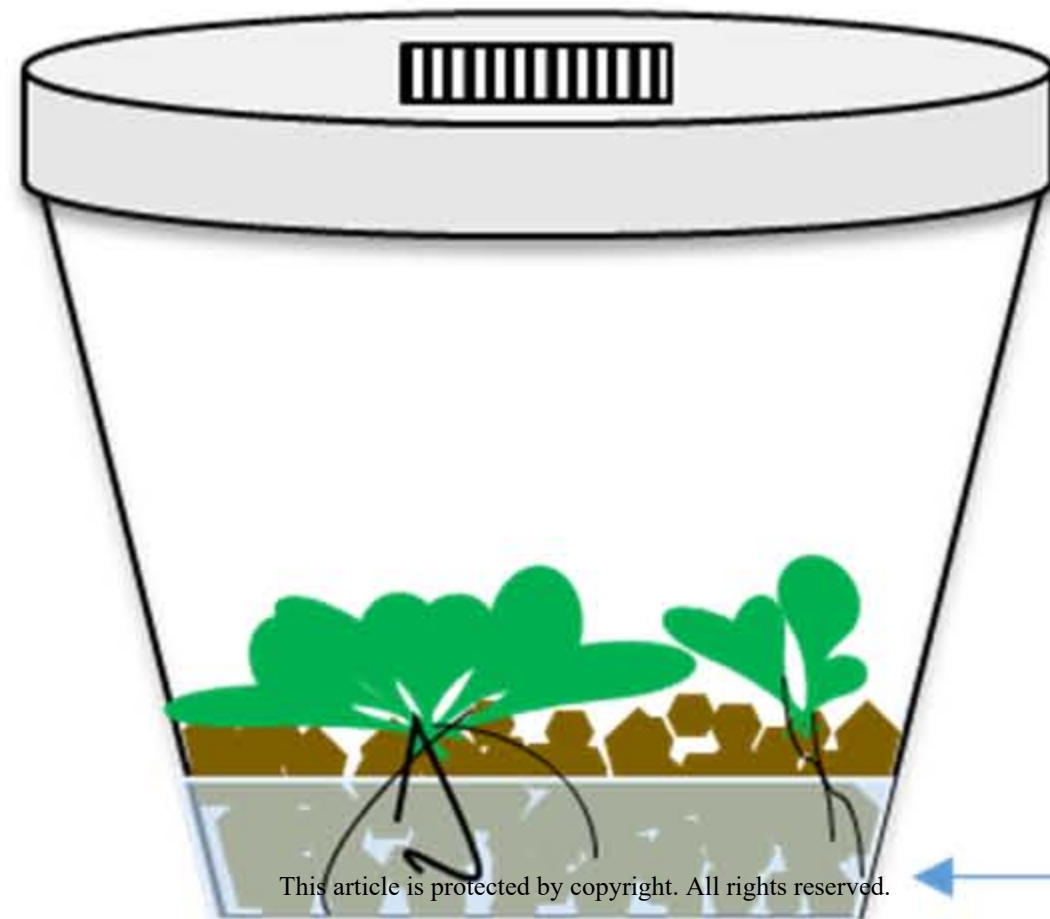


B

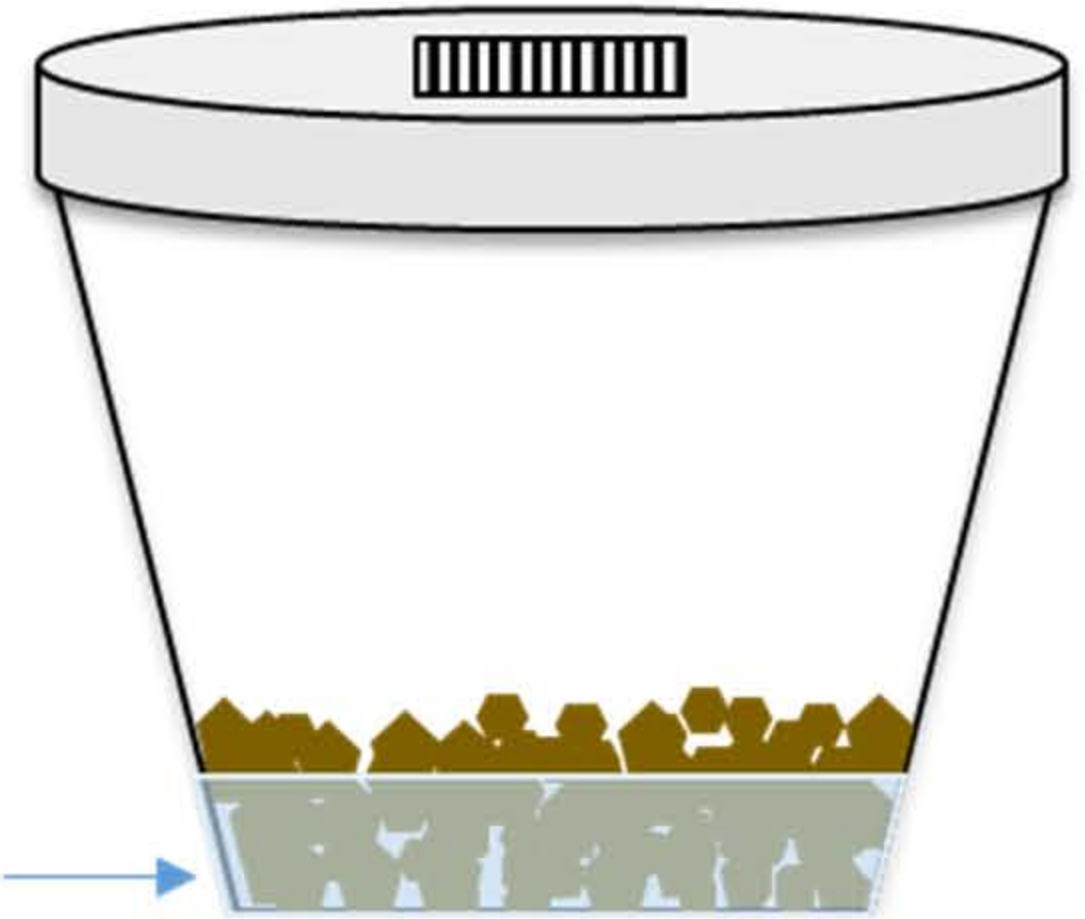


Soil suspension

C



D



Mock solution

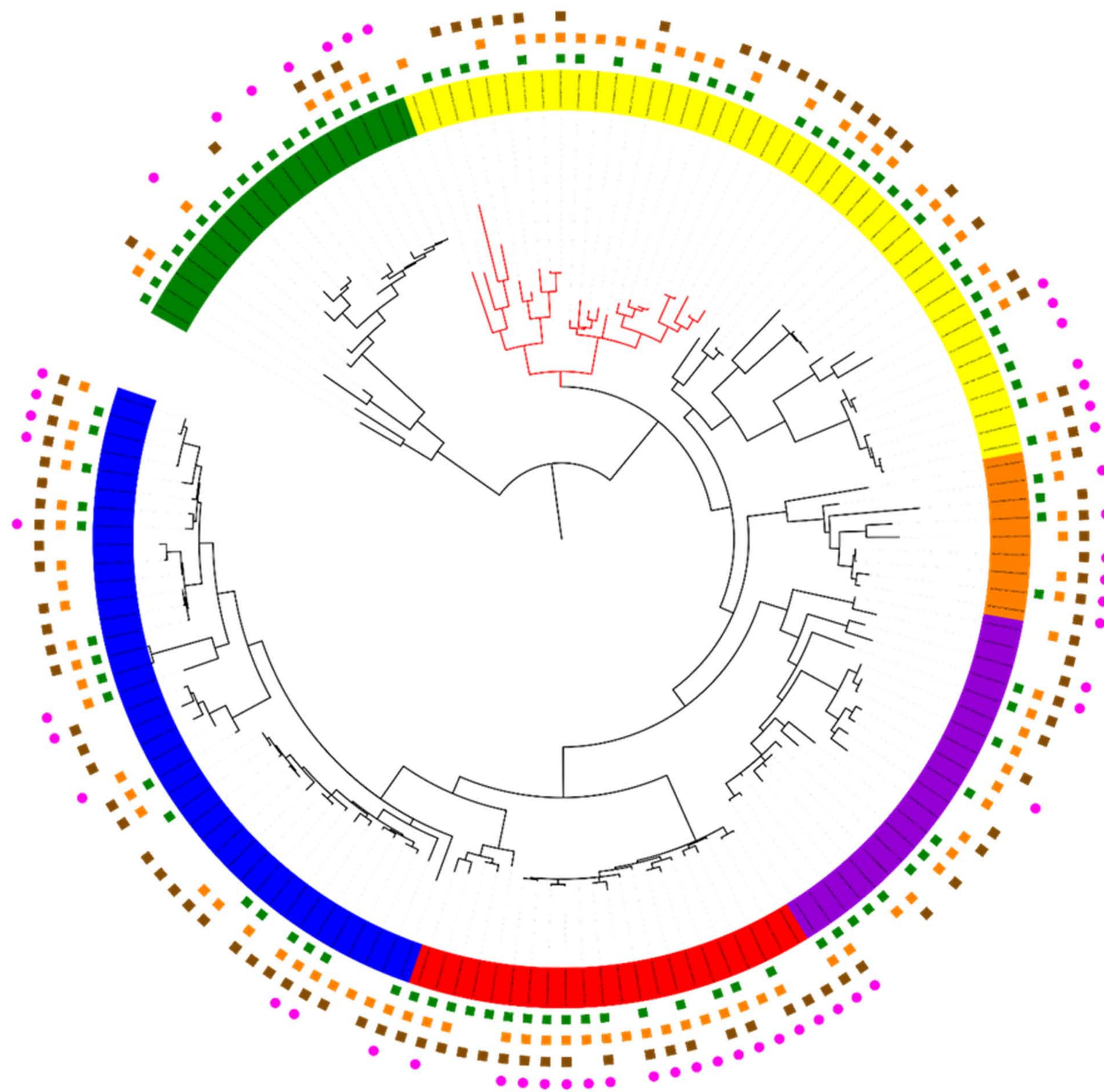
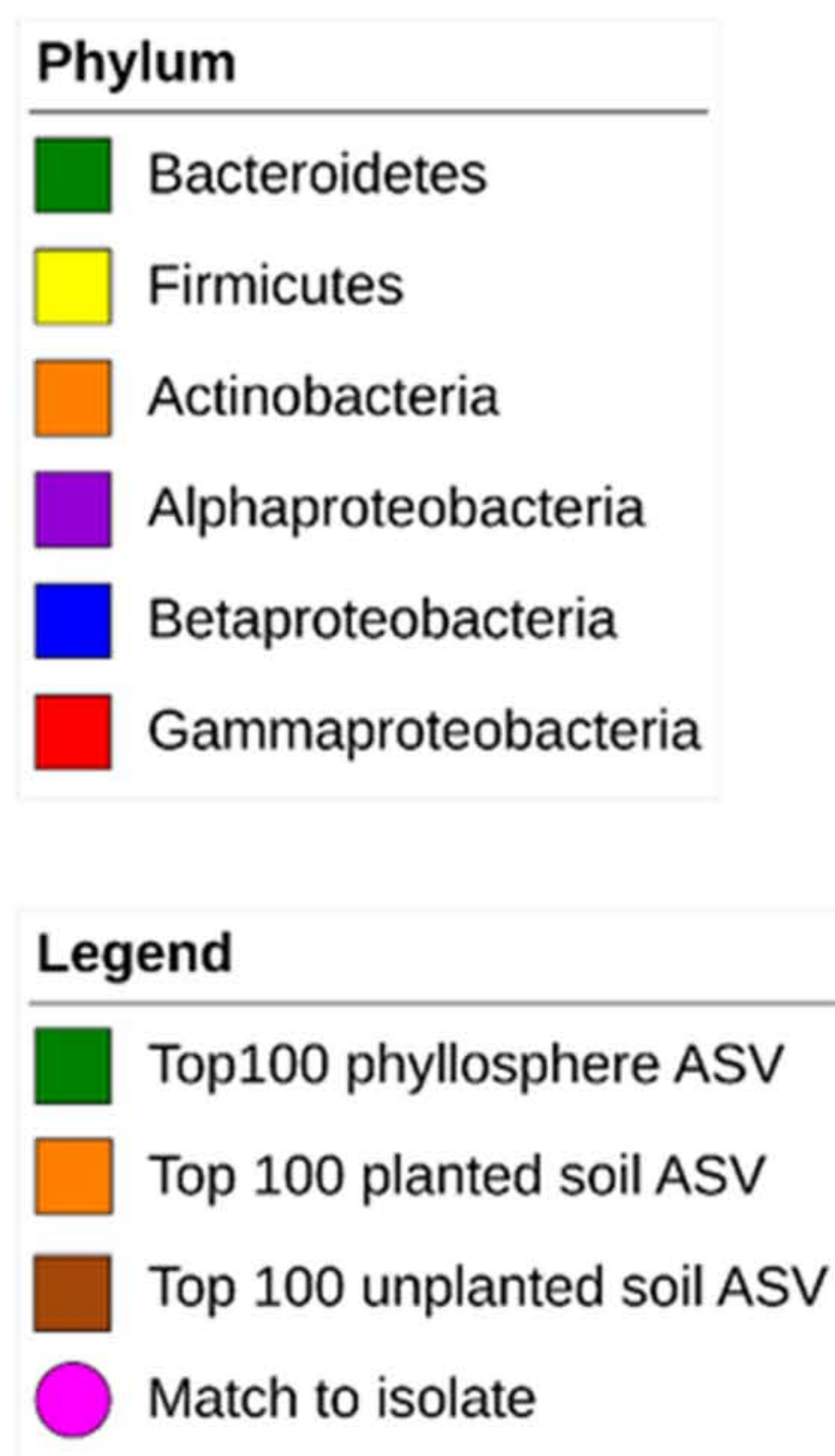
Tree scale: 1 

Figure 2

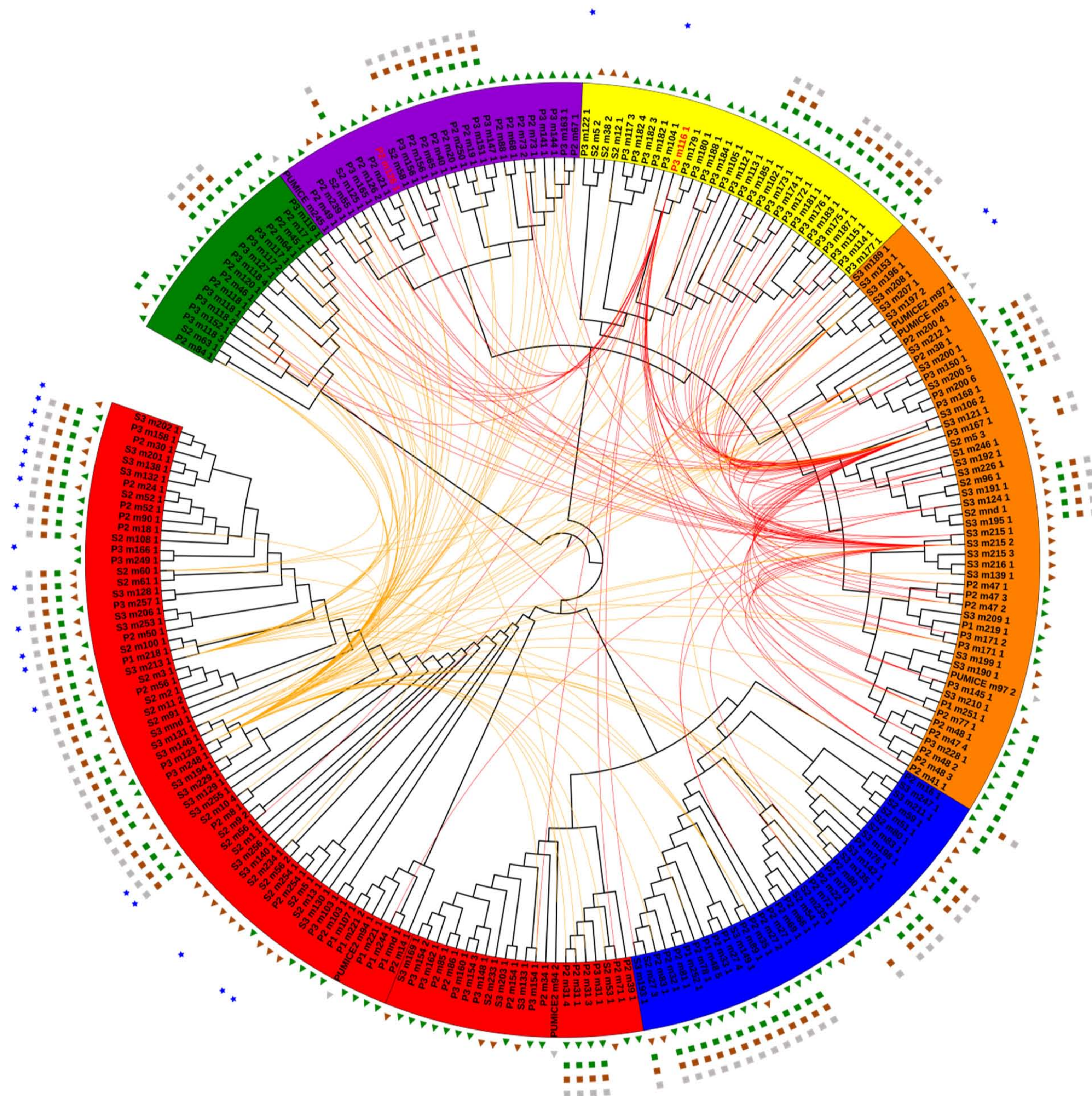
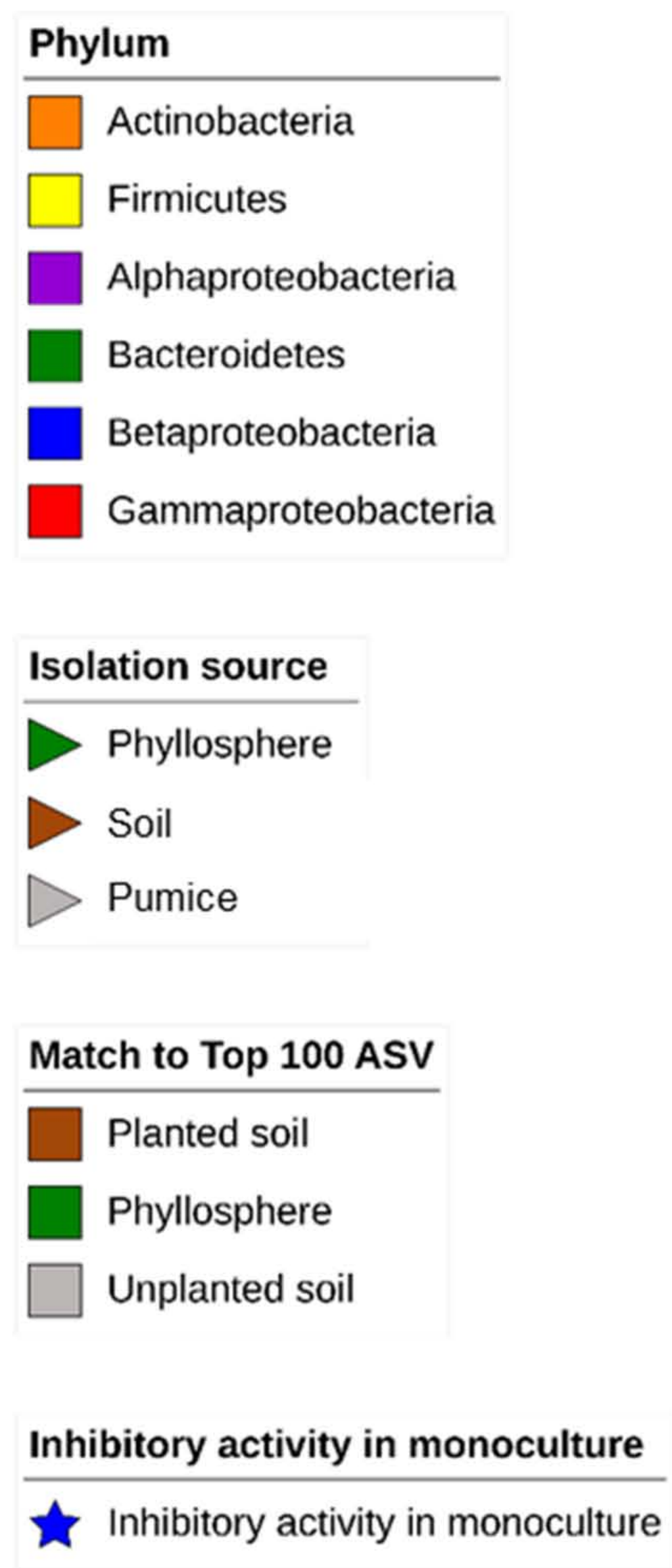
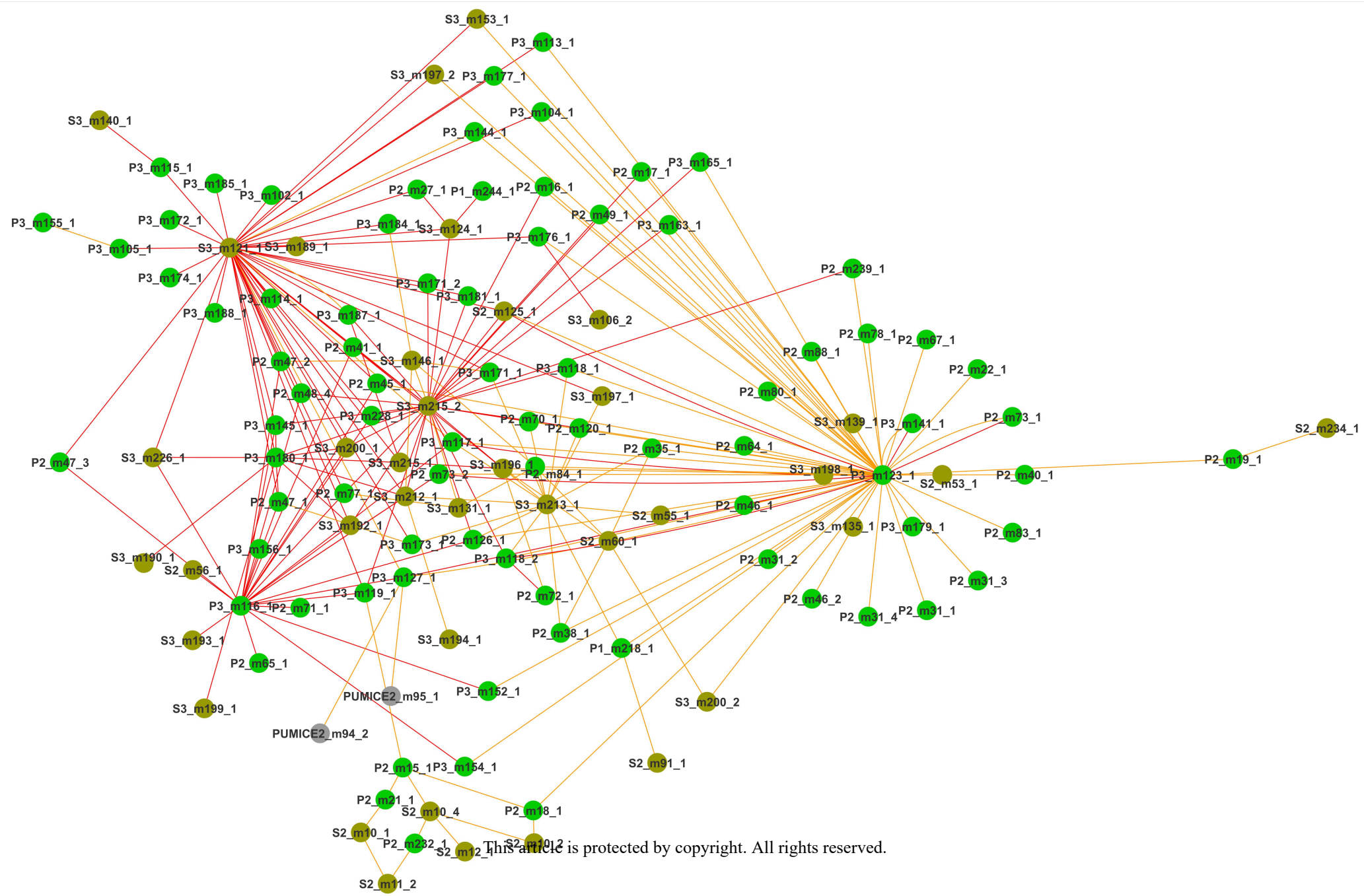


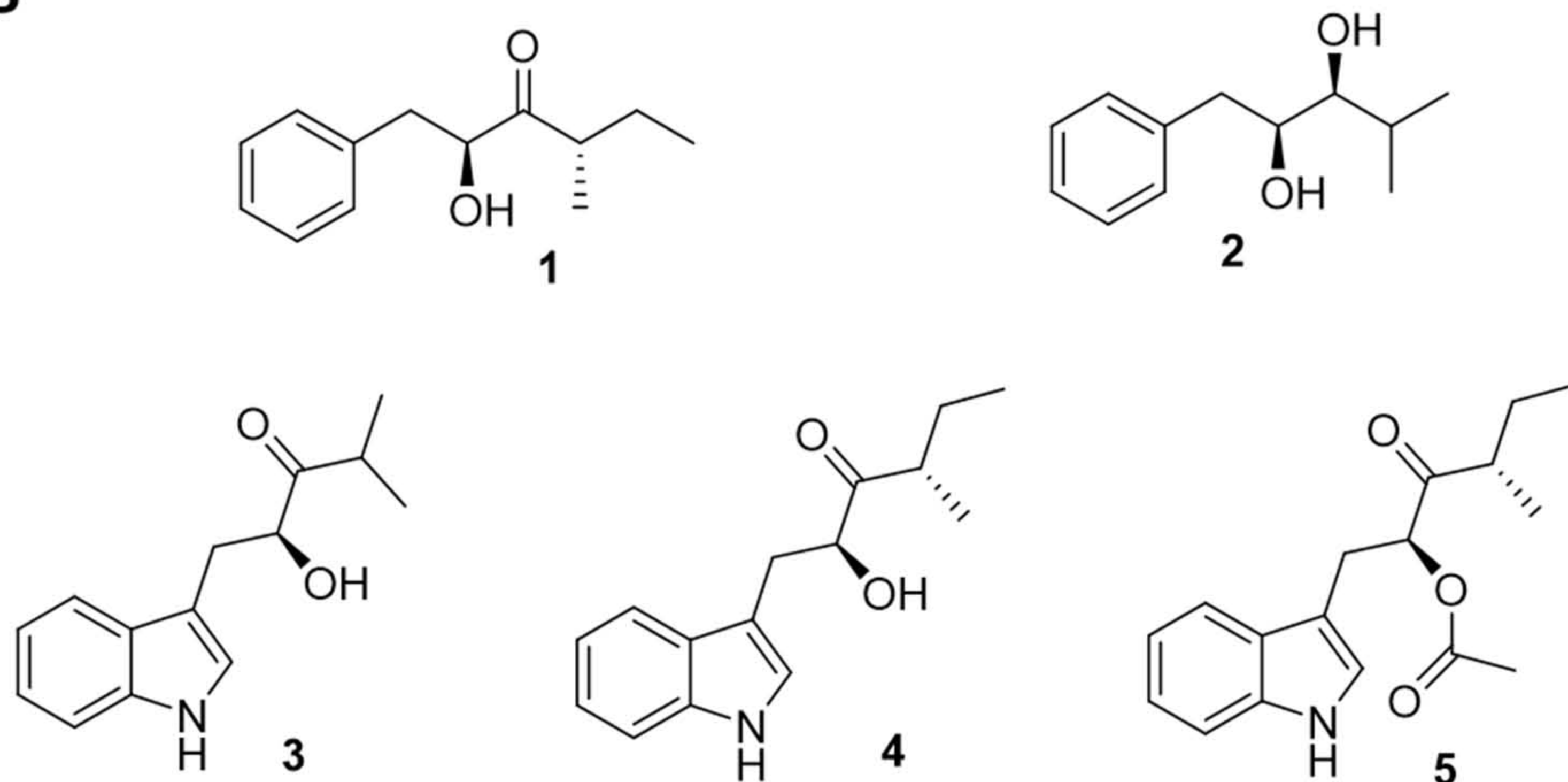
Figure 3



A



B



locus tag	Accession number	Annotated Function	size (AA)
GC101_RS07275	WP_171716831.1	thiamine pyrophosphate-binding protein	547
GC101_RS07280	WP_171716701.1	carboxymuconolactone decarboxylase family	122
GC101_RS07285	WP_171716702.1	hypothetical protein	116
GC101_RS07290	WP_171716703.1	ketoacyl-ACP synthase III	330